

**SCHOOL OF GRADUATE STUDIES
KWAME NKRUMAH UNIVERSITY OF SCIENCE AND
TECHNOLOGY, KUMASI, GHANA**

**GEOSTATISTICAL METHODS FOR ESTIMATING IRON,
SILICA AND ALUMINIUM WITHIN IRON ORE DEPOSITS:
-A CASE STUDY OF THE MOUNT TOKADEH STUDY AREA, YEKEPA,
YARMEIN DISTRICT, NIMBA COUNTY, REPUBLIC OF LIBERIA**

BY

**EMMANUEL ALLEN DONSEAH
(BSC. CIVIL ENGINEERING)**

**THE THESIS SUBMITTED TO THE DEPARTMENT OF GEOMATIC
ENGINEERING,
COLLEGE OF ENGINEERING
IN PARTIAL FULFILMENT OF THE REQUIREMENT FOR THE DEGREE
OF
MASTER OF SCIENCE**

OCTOBER 2016

DECLARATION

I best of my knowledge, it contains no material previously published by another person, nor material which has been accepted for the award of any other degree of the University except hereby declare that this submission is my own work towards the award of MSc and that, to the where due acknowledgement has been made in the text.

EMMANUEL A. DONSEAH

Signature

Date

(Student & ID)

(PG2233414) **Certified
by:**

Prof. ALFRED A. DUKER

Signature

Date

(Supervisor)

REV. JOHN AYER

Signature

Date

(Supervisor)

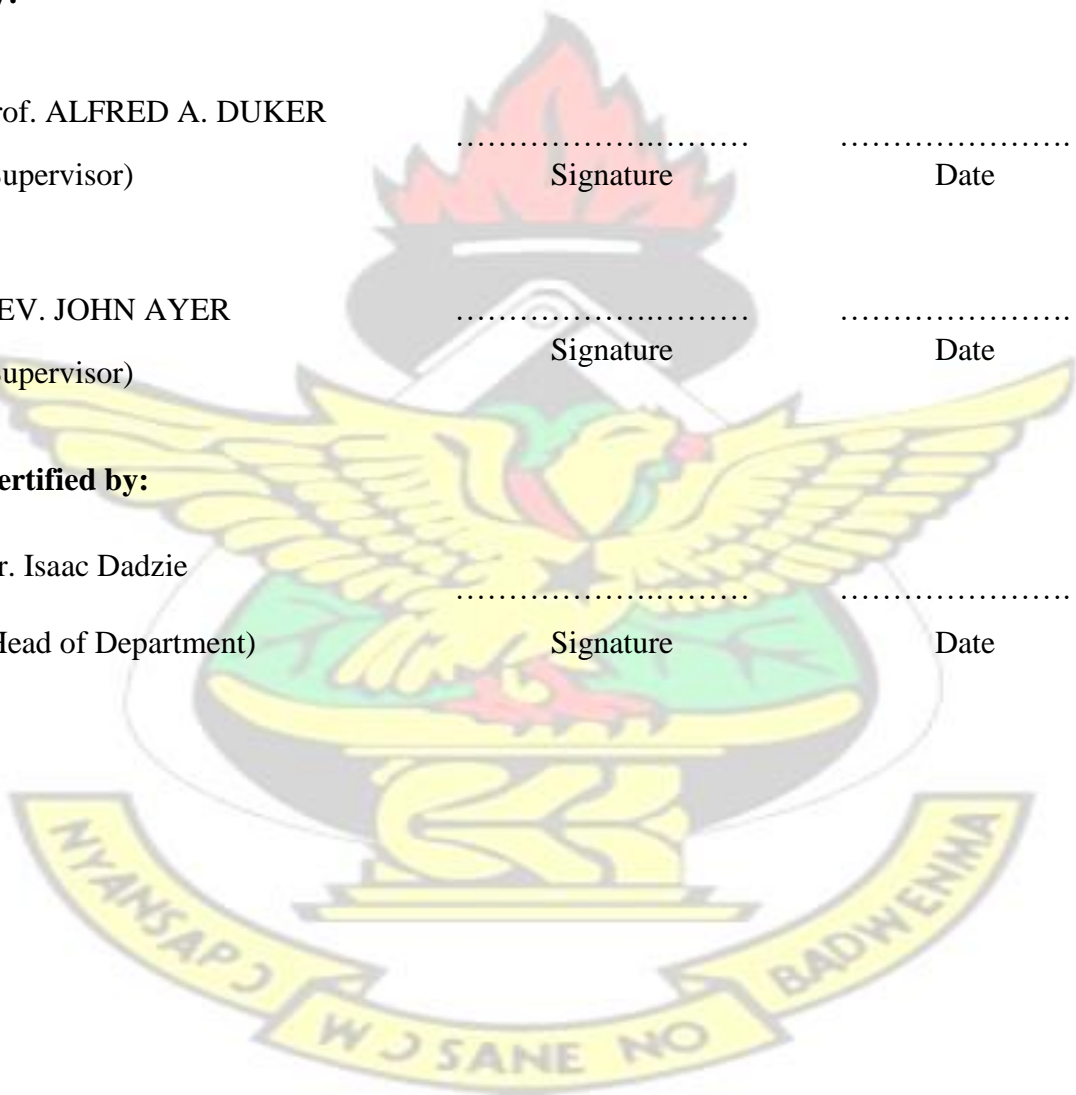
Certified by:

Dr. Isaac Dadzie

Signature

Date

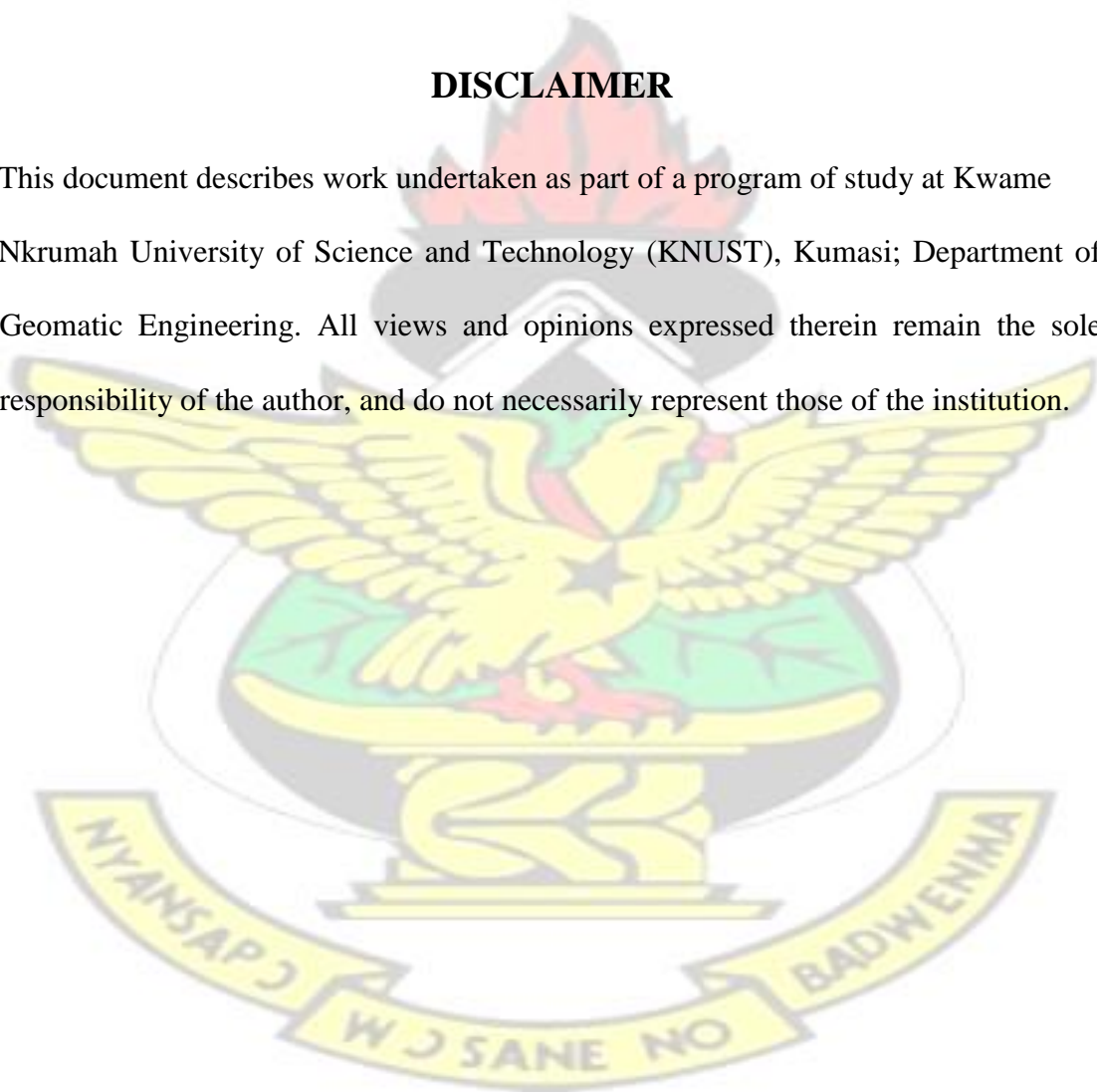
(Head of Department)



KNUST

DISCLAIMER

This document describes work undertaken as part of a program of study at Kwame Nkrumah University of Science and Technology (KNUST), Kumasi; Department of Geomatic Engineering. All views and opinions expressed therein remain the sole responsibility of the author, and do not necessarily represent those of the institution.



ABSTRACT

Mining history in Liberia is often plagued with difficulties of uncertainty of commercial quality and quantity of mineral existence in a particular region. Previous studies conducted at Mount Tokadeh, study area which lies between latitude $7^{\circ}15'N$ and $7^{\circ}45'N$ and longitude $8^{\circ}15'W$ and $8^{\circ}45'W$ was distributed in three ore zones; the Oxide Ore, Transitional Ore and Primary Ore. It was also proven that there is some considerable amount of silica and alumina in this ore deposit but the extent of these impurities within this ore deposit were unknown.

The main aim of this research was to investigate the use of information gain from kriging interpolation techniques (Ordinary Kriging, Indicator Kriging and Universal Kriging) to estimate iron ore resources and categorize selective mining unit as High Grade Ore (HGO) or Direct Shipping Ore (DSO).

Field data were processed in excel template and exported into shapefile format inputted into ArcGIS/Arcmap 10.2.1 for interpolation using three main kriging interpolators. Four classes of creative colors were used to delineate the relative quality of mineral distribution within mining site. The final output maps (Prediction map, Probability map and Error of Prediction map) were obtained. Voxler was used to model borehole data in 3D format and was overlaid on the output kriged map for validation. The results showed that Indicator Kriging which uses threshold was the best interpolation method that categorizes the various mining units. Integrated method using Kriging in GIS was introduced and implemented in this work to determine the prospect of using this approach in mapping the spatial division of iron, silica and aluminum content and tonnage of iron ore.

ACKNOWLEDGEMENTS

I am most grateful to the Almighty God whose divine favour and blessing has brought me this far. My sincere gratitude also goes to these following institutions and personality for their contributions in ensuring that this research was a success.

To Prof Alfred Allan Duker and Rev. John Ayer, Professor and Senior Lecturer at the Department of Geomatic Engineering, KNUST for their good supervisory skills, dedications, encouragements and timely comments. They have, during the course of this thesis, provided inputs, guidance and immense valuable feedbacks. They have been exemplary, as an academic role model to me, upholding the true spirit of science and academic research. They have also assisted me in becoming properly familiar with the relevant engineering background knowledge, vital to the completion of this thesis.

My profound thanks and appreciation to the CEO and managing staff of ArcelorMittal Liberia. The company that made me realized my dream. May God continue to bless and prosper your businesses around the World.

Special appreciation to Mr. Marcus Wleh, Corporate Responsibility Manager, and his ArcelorMittal Liberia office staff including Mr. Eric Swen for their tireless effort in making sure that we remain in school, well accommodated and special attentions given to us by the school authority.

Special thanks and appreciation to my dear wife, Annie Brewer and children Bless Emmanuelyn Donseah, Emmanuel Success Donseah, Elyn Donseah, Allen Favour Donseah and Elizabeth Divine Donseah for their support and strong prayer that kept me strong in the course of the study. God bless you all.

TABLE OF CONTENTS

DECLARATION	ii
DISCLAIMER	iii
ABSTRACT	iv
ACKNOWLEDGEMENTS	v
TABLE OF CONTENTS	vi
LIST OF TABLES	viii
LIST OF FIGURES	ix
LIST OF ABBREVIATION AND ACRONYMS	x
CHAPTER 1	1
INTRODUCTION	1
1.1 BACKGROUND	1
1.2 Problem statement.....	2
1.3 Aim and Objectives.....	2
1.3.1 Main Aim	2
1.3.2 Specific Objectives.....	2
1.4 Scope of current work	3
1.5 Relevance of research	3
1.6 Structure of Thesis	3
CHAPTER 2 ORE DEPOSIT CLASSIFICATIONS AND GEOSTATISTICAL	4
INTERPOLATION TECHNIQUES	4
2.1 Ore Deposit Classifications.....	4
2.1.1 Igneous Ore	6
2.1.2 Metamorphosed Iron ore formations.....	6
2.1.3 Sedimentary Ore.....	7
2.2 Iron Bearing Minerals	7
2.2.1 Magnetite.....	8
2.2.2 Hematite	8
2.2.3 Hydrous Iron Oxide.....	8
2.2.4 Ilmenite.....	9
2.2.5 Siderite	9
2.3 Deleterious Elements in iron ore.....	9
2.4 Geostatistics	10
2.4 Interpolation Methods	15

2.4.1 Inverse Distance Weighting (IDW) Method	16
2.4.2 Triangulated Irregular Network (TIN) method	16
2.4.3 Polygon method.....	16
2.4.4 Multiquadratic Technique	17
2.4.5 Natural Neighbor.....	17
2.5 Kriging Methods of Geostatistical Interpolation.....	17
2.5.1 Variography in Kriging	18
2.5.2 Ordinary kriging.....	19
2.5.3 Indicator kriging.....	21
2.4.3 Universal kriging (UK)	23
2.6 Geographic Information Systems (GIS).....	25
CHAPTER THREE.....	26
MATERIALS AND METHODS.....	26
3.1 The Study Area	26
3.1.1 Geology	27
3.1.2 Climate	29
3.1.3 Local Population	29
3.2 Materials	29
3.2.1 Sampled Data	29
3.2.2 Other Materials.....	31
3.3 Methodology.....	32
3.3.1 Geostatistical data analysis.....	34
3.3.2 Voxler.....	37
CHAPTER 4.....	38
RESULTS AND ANALYSIS	38
4.1 Results.....	38
CHAPTER 5.....	56
CONCLUSION AND RECOMMENDATION.....	56
5.1 Conclusion	56
5.2 Recommendation	57
REFERENCES	58

LIST OF TABLES

Table 2.1: Selected Geologic Ages of Iron Ore Deposits	6
Table 2.2 Chief Iron Bearing Mineral	8
Table 3.1: Drill hole data	32
Table 3.2: Summary of Data Extracted from drill hole database use in model for interpolation	32
Table 4.1: Statistical concentration analysis result of Iron, Silica and Alumina	41
Table 4.2: Prediction Errors Ordinary Kriged result	42
Table 4.3: Prediction Error Indicator Kriged result.....	42
Table 4.4: Prediction Error Universal Kriged result	43



LIST OF FIGURES

Figure 2.1: Principle of ordinary kriging	20
Figure 2.2: Threshold of a variable in space	22
Figure 2.3: Principle of indicator kriging	22
Figure 2.4: Principle of Universal Kriging	24
Figure 3.2: Google earth image of Tokadeh Mining Site	28
Figure 3.3: Design of work flow	34
Figure 3.4: Searching neighborhood	36
Figure 3.5: Cross validation	37
Figure 3.6: Method Report	37
Figure 4.1: Semivariogram of Iron (Fe) distribution (Ordinary Kriging)	39
Figure 4.2: Semivariogram of Iron (Fe) distribution (Universal Kriging)	40
Figure 4.3: Semivariogram of Iron (Fe) distribution (Indicator Kriging)	40
Figure 4.4: Histogram showing statistical result of iron (Fe) distribution in kriging .	41
Figure 4.5: Normal QQPlot	43
Figure 4.6: Ordinary Kriged Prediction	46
Figure 4.7: Indicator Kriged Prediction	47
Figure 4.8: Universal Kriged Prediction Map	48
Figure 4.9: Ordinary Kriged Probability Map.....	50
Figure 4.10: Indicator Kriged Probability Map	51
Figure 4.11: Universal Kriged Probability Map.....	52
Figure 4.13: Indicator Kriged Standard Error	54
Figure 4.14: Universal Kriged Standard Error	55
Figure 4.15 Alumina distribution map	56
Figure 4.17: 3D view of the bore holes	58

LIST OF ABBREVIATION AND ACRONYMS

DSO	Direct Shipping Ore
EPA	Environmental Protection Agency
GDP	Gross Domestic Product
GIS	Geographic Information System
HGO	High Grade Ore
IDW	Inverse Distance Weighting
IK	Indicator Kriging
MFA	Ministry of Foreign Affairs
MLME	Ministry of Lands, Mines and Energy
OK	Ordinary Kriging
TIN	Triangulated Irregular Network
UK	Universal Kriging
USA	United States of America



CHAPTER 1

INTRODUCTION

1.1 BACKGROUND

Before 1989, Liberia was the world's sixth largest exporter of iron ore which was contributing to as much as 64% of total exports and 25% Gross Domestic Product (GDP). However, there has been no production until 2003, making the iron ore sector a prime mover for economic growth (Chadwick, 2011).

Liberia's mineral development policy and mining code envisaged that exploitation would be balanced appropriately with sustainable environmental preservation (MLME, 2010). Other laws governing the mining sector in Liberia, particularly the National Environmental Protection Agency of Liberia's Environmental Protection and Management Law, (2002) required a mandatory environmental impact assessment prior to exploitation (MFA, 2003), and the facilitation of conservation of the biological diversity of Liberia. These require the use of knowledge driven exploitation of minerals in order not to degrade the land in search of such, at places without a high probability of ore finds.

Geostatistical methods and Geographic Information Systems can provide the necessary tools for ensuring knowledge-based and targeted exploitation.

Geostatistics uses spatial and temporal patterning to exploit the relationships that help to model potential values of a variable at unsampled points, and these analyzed in GIS, would limit the search of minerals to areas with high probability of mineral ore occurrences.

1.2 Problem statement

The mining industry is often plagued with difficulties mainly due to uncertain existence of the prospected mineral of interest in commercial quantities, the grade and tonnage available and the exact location within a region where minerals are likely to be found. Previous studies conducted in the study area show that ore deposits are distributed in three ore zones (Oxide, Transition and Primary ore zones) (Amikiya, 2014). It was also established that iron concentration increases with decreased silica content in all the ore zones. However, the distribution of iron, silica and alumina in the three ore zones is not known. The applications of geostatistics method can provide a means of estimating both the grade and tonnage of the various grades at unsampled points together with estimated errors. This would reduce the uncertainty or investment risk and helps control the number of exploration drilling requirement as well as establishing decisions to mine based on grade and tonnage.

1.3 Aim and Objectives

1.3.1 Main Aim

The main aim is to investigate the use of information gained from Indicator Kriging (IK), ordinary Kriging (OK) and Universal Kriging (UK) in estimating Iron Ore resources and apply the best method to categorize selective mining unit as High Grade (HG) or Direct Shipping Ore (DSO).

1.3.2 Specific Objectives

The specific objectives are to:

1. Use an integrated methodology of Kriging in GIS to demonstrate the possibility of mapping the spatial distribution of iron, silica and alumina in the ore deposit of the Tokadeh Study area.

2. Delineate the relative magnitudes (tonnages) using creative colors to each mineral type at various locations of the study area.
3. Prepare Prediction maps, Error of Prediction maps, Quantile maps, Probability maps and sampling point map for these mineral deposits using GIS.

1.4 Scope of current work

This work is limited to Mt. Tokadeh concession area of Liberia. The integration of geostatistics and GIS is used to predict the mineral distribution of Tokadeh ore deposits using sampled data collected from 110 drilled bore holes. There are several geostatistical interpolation methods, but in this research, the kriging procedures of interpolations (indicator kriging, ordinary kriging and universal kriging) were used based on the phenomena being studied. Variography is first done to determine which mathematical method is best.

1.5 Relevance of research

The unavailability of estimated ore reserve grades and quantities prior to mining have led to the failure of mining projects and unnecessary degradation of biodiversity even where no ore exist (Dimitrakopoule, 2012). The results of this effort would facilitate decisions on deposit viabilities at different locations in terms of quality and quantity.

1.6 Structure of Thesis

This research is compiled into 5 chapters.

An introduction presented in chapter one includes background, problem statement, objectives, scope of current work, and relevance of research.

In Chapter 2, a review of ore deposit classifications in terms of mineral burden, geostatistical techniques and use in mineral prediction and exploration are made. This

chapter further includes challenges of interpolation methods and their relative strengths and weakness.

The material and methodology employed in the current study is presented in chapter 3. The results of current effort are in chapter 4. The chapter also includes a discussion of these results and deduction made from these analyses.

The conclusions drawn from the study are presented in chapter 5 together with some recommendations for further studies

CHAPTER 2 ORE DEPOSIT CLASSIFICATIONS AND GEOSTATISTICAL INTERPOLATION TECHNIQUES

2.1 Ore Deposit Classifications

Iron constitutes 2 to 3% of the earth crust in sedimentary rock and up to 8.5% in basalt and gabbro. For an iron ore to be considered economically worthwhile, it should contain at least 25% of iron concentration (Amikiya, 2014).

There are over 300 iron bearing minerals that contain some percentage of iron but only the following five are key economic sources of iron ore:

1. Hematite (Fe_2O_3)
2. Goethite ($\text{Fe}_2\text{O}_3\text{H}_2\text{O}$)
3. Pyrite (FeS_2)
4. Magnetite (Fe_3O_4)
5. Siderite (FeCO_3)

Among these, magnetite and goethite are the chief sources due to their high concentrations of iron (U.S EPA, 1994). Mineral resources are made up of three main

classifications, namely; indicated or inferred resources, measured, and reflecting diminishing levels of geological confidence.

Mineral resource classification ought to take into account applied consideration such as drill-hole spacing, geological control and continuity, drilling, sampling and assay integrity, grade continuity, block size, estimation method and potential mining method and reporting epoch. Major reflection is also drawn to metallurgical factors, cut-off grades, mining and or assumption, cost and revenue factors, market assessment and risk factors such as environmental, social or political (Everett, 2013).

Iron ore classifications may be based on geological formation. Iron ore consist of a wide range of rock history and the physical earth's crust as well as the wide range of land-area-based distribution. Iron ore originated in primitive rock of the earth's layer with ages over 2.5 billion years. Rock unit are molded in different land and rockbased ages (Poveromo et al., 2000). Table2.1 Exhibits the selected geologic age of iron deposits in geologic history.

Table 2.1: Selected Geologic Ages of Iron Ore Deposits

Geologic Age	Deposit	Location
Paleozoic Era		
PERMIAN PERIOD	Damuda Sandstone (Hematite)	India
Pre-Cambrian Era	Nimba Range Hematite	Liberia
	Minas Gerais Serra dos Carajas Hematite	Brazil
	Krivoi Rog Hematite	Ukraine, Russia
	Bihar, Orissa and Mahya-Pradesh Hematite	India
	Labrador Hematite	Quebec and Labrador
	Lake Superior Taconite and Jaspilite, Hematite and Magnetite	Michigan, Wisconsin,
		Minnesota, Ontario
	Kirunavaara Magnetite	Sweden
	Cerro Bolivar and El Pao Hematite	Venezuela
	Hamersley Range Hematite	Western Australia
Oligocene Epoch	Cheikh-ab-Charg Hematite	Iran
Mesozoic Era		

Cretaceous Period	Salzgitter Limonite and Hematite Algeria and Moroccan Hematite and Magnetite Bilbao Hematite	Germany North Africa Spain
Jurassic Period	Iron Spring Magnetite Minette, Limonite and Hematite	Utah Germany, France
Triassic Period	Kasmir Calcareous Iron Ore (Hematite)	India

Cenozoic Era

Tertiary Period		
Pliocene Epoch	El Tofo Magnetite Kerch Oolitic Limonite	South America, Chile Russia, Crimea
Oligocene Epoch	Cheikh-ab-Charg Hematite	Iran
Eocene Epoch	Bahariya Hematite Upper Assam Clay Ironstones	Egypt India

(Source: Poveromo et al. 2000, "Iron Ores", Chapter 8, pp.3)

The geological surrounding of iron ore mostly originated in igneous rock (created in a volcano), metamorphic, or sedimentary (coming from material sink in liquid) rock, or as a weathering product of other most important iron bearing materials. According to Poveromo et al. (2000), iron ore are classified according to their geological structure, occurrences, arrangement and similarity into igneous ore, metamorphic ore formation and sedimentary ores.

2.1.1 Igneous Ore

These originated from crystallization of moisture materials containing rock strata of huge iron percentage settlement as they become clear and real to form iron-rich concentrates. Igneous ores are often high in iron content but may also contain high phosphorus or titanium content. (Poveromo et al., 2000)

2.1.2 Metamorphosed Iron ore formations

These are transmuted bedded rusty rocks sedated typically of sporadic thin layers of ferric oxides and chert or fine-grained quart. This type of iron is characteristically exhibited in the mineral form of hematite or magnetite, in addition to lesser quantity of silicate and carbonates irons. All of the Pre-Cambrian sedimentary iron structures are

of this type. They contain the magnetite and nonmagnetic taconites of Minnesota. Metamorphosed iron ore also consist of ones in which the primary structure of the ore had been concealed by wide-ranging recrystallization.(Poveromo et al., 2000)

2.1.3 Sedimentary Ore

These can be made up of siderite, silicate, Oolites of hematite, iron and limonite among others in the mold of calcite, silicate or siderite and usually has large range of locational arrangement concordant with other sedimentary rocks. Sedimentary ore normally accommodate phosphorus content and may be self-fluxing.(Poveromo et al., 2000)

2.2 Iron Bearing Minerals

There are over 300 minerals which accommodate some percentage of iron, though, entirely a small number contain a marketable content of iron. Those minerals comprising commercial quantities of iron are arranged into their chemical composition, carbonate, oxides, silicate and sulfides.

In table 2.2, the carbonate and oxide classes are shown and specified those mineral species that are generally considered commercial iron bearing mineral.

Table 2.2 Chief Iron Bearing Mineral

Class and Mineralogical name	Chemical Composition of Pure Mineral	Common Designation
Oxide		
Imenite	FeTiO_3	Iron-titanium Oxide
Hematite	Fe_2O_3	Ferric Oxide
Magnetite	Fe_3O_4	Ferrous-Ferric Oxide
Limonite	FeO_2 FeO(OH)	
Carbonate		

(Source: Poveromo, J.J. et al., 2000. "Iron Ores". Chapter 8, pp.547–642).

2.2.1 Magnetite

This has a structure Fe₃O₄, with iron content of 72.36%. It contains dark gray to black color. Strongly magnetic, it sometimes maintains polarization to act as a natural magnet. Magnetite is normally formed in metamorphic, igneous and sedimentary rocks (Hussain, 1985; Podolosky and Keller, 1994).

2.2.2 Hematite

This has a chemical arrangement of Fe₂O₃, with iron content ranging from 65- 69.94%. It contains colors that range from dull red to bright red and steel gray. Its diversities are known as martite (pseudomorphic after magnetite), reflective, crystalline, maghemite (magnetic ferric oxide), ocherous, earthy and compact. According to Hussain (1985), Podolosky and Keller (1994) hematite has wide occurrences in many types of rocks and is of changeable origin. Hematite can also be found with trace deposits in sedimentary and metamorphic, as well as an output of the natural disintegration of magnetite.

2.2.3 Hydrous Iron Oxide

This is mineralogically called Limonite and is made up of several combinations of several minerals lepidocrocite or goethite. The chemical formula for goethite is HFeO₂, containing 62.85% iron. However, Lepidocrocite with a chemical composition of FeO(OH) is extraordinarily brown or yellow to approximately black in color, additionally condensed to earthy and ocherous. The word limonite signifies unfamiliar oxides with inconsistent water percentage as a result of water vein or high concentration. It is a less important mineral, made customarily by natural disintegration

of mineral due to erosion among others, likewise develops in combination alongside other sedimentary and oxide rocks.

2.2.4 Ilmenite

This is of a natural configuration of FeTiO_3 , with a conforming 36.80% iron. It is also considered as iron titanate. Generally ilmenite which is correlated with magnetite is customarily mined as titanium source rather than iron with iron being recovered as a by-product.

2.2.5 Siderite

This is composed of a chemical formation of FeCO_3 with 48.20% iron as well as color ranging from white to brown and greenish gray. This mineral constitutes only a limited portion of the total world reserves. Siderite has variable aggregate of calcium, magnesium or manganese. It differs from heavy, fine grained and compressed to crystalline. Siderite ore is sometime characterized as black band ore or spathic ore.

Siderite is one of the valuable adsorbent of natural raw materials (Drolq et al., 2015)

2.3 Deleterious Elements in iron ore

The chemical parts of iron minerals are either compounds such as oxides-silica, alumina, lime, and magnesia; or as elements such as sulfur, phosphorus, manganese, titanium, chromium, and nickel. Most of these elements which are largely called impurities have deleterious effects though others are advantageous. The main deleterious elements are phosphorus and sulfur. They are to be reduced to acceptable amounts in smelting processes to determine the marketability of ores (Carr & Dutton, 1959).

Silica (SiO_2) is continuously existent in iron ore. However, large amount of silica are slagged off in the course of the extraction of silica from ore body (smelting). At

temperatures above 1300 degree Celsius few will be condensed and form an alloy with the iron. Silicon presence will increase in the ore body when the furnace is hotter.(Kiptarus et al., 2015)

Phosphorus (P) is one of the major impurities which at high levels in steel reduce the strength of steel making it brittle and easily crack. Due to these factors, in steel making, chemical and biological procedures are used to remove phosphorus from iron ore. Phosphorus is either integrated into the crystal lattice of iron oxides or into the gauge mineral. It has a harmful outcome on the viability of steel. So many Phosphorus enriched ores are unmarketable around the world leaving many iron ore mines abandoned. Acceptable phosphorus concentration in iron ore should be less than 0.08%.(Carr & Dutton, 1959)

Sulphur is one of the major impurities that mostly increase cost of ironmaking. Sulphur mostly enters the ironmaking process from coke used as fuel, even though; some iron has high Sulphur content. Pretreatment is usually carried out to remove or reduced the level of sulfur content present in an iron ore body. When refining iron to steel, it is necessary to remove or reduce the level of sulfur in the iron (Hussain, 1985).

Aluminium is one of the major harmful metallic elements found within iron oxide. It affects the strength of steel making. According to Shakhashiri (2008), alumina is the predominant metal and the third bountiful element in the earth's crust and due to its chemical reactiveness it combines with over 270 different minerals with its chief ore being bauxite and iron oxide.

2.4 Geostatistics

Geostatistics is a subdivision of statistical science that analyzes temporal and spatial phenomena and exploits on the spatial relationship that form credible values of

variable(s) at an un-sample location. In simple term, geostatistics studies phenomena or occurrences that vary in space and time (Bohling, 2005a). Geostatistics is used to select, and block map underground ore bodies for mining decisions (Ver Hoef, 2002).

Everything on the surfaces of the earth or underneath the surface including the distribution of minerals has a definite spatial location. The distribution of such natural phenomena may form spatial patterns which are explainable in Tobler's law that "everything is related to every other thing but near things are more closely related". Tobler's law shows that objects in a particular location can influence their neighborhood in term of distributions and patterning.

Estimation of ore reserves had used different predictable interpolation methods in different areas such as the Triangulated Irregular Network (TIN), Inverse Distance Weighting (IDW) and Polygon methods, etc., in addition to contemporary procedures like Multiquadratic techniques, natural neighbor interpolation and kriging.

These interpolation techniques are mathematical approaches employed to a dataset of inconsistent distribution, and help obtain values for the variable of interest at unsampled locations established on neighboring computation (Bohling, 2007). This idea is mainly based on the usage of appropriate functions that ties the spatially distributed data to determine a normal calculation function. Contingent on the precision of interpolated estimate gave significant saving in time and costs which could be realized by limiting search to only places of probability of occurrences. The method may also integrate some attenuation functionality so that it ought to be conceivable to know how far from the source location a particular find can go.

George Matheron (1971) industrialized Geostatistics at the Centre de Morophologie Mathematicque ai Frontainebleau, France. The principal focus of geostatistic was

evaluating ore grade in reach in a mine. This principle is nowadays applicable to various areas in geology and other scientific disciplines as well as in medicine.

The kriging method has been used in the mining industries as the most precise and dependable method for prediction and reserve estimation. However experience was needed to choose the most applicable kriging method for application (Saleem, 2007).

The usage of integrated methods such as IK, OK, and UK techniques in GIS help aid mining resolution to control and strategized ore production.

The most unique quality feature of geostatistics is to employ regionalized variables, that are variables that lies between deterministic and random variables. Regionalized occurrences may display spatial continuousness. Nevertheless, since it is not at all times feasible to sample the entire area of interest, values of unsampled points have to be calculated from data taken at definite locations with known X and Y coordinates that can be sampled and then used in kriging. The unidentified sampled region prediction is strongly influenced by the location of samples, shape, spatial structure size and orientation. Regionalized variable evaluation and sampling are done to establish a standard of variation in the phenomenon under scrutiny that can be mapped as a “contour” for the geographical locality.

Geostatistics is analyzed subsequently as follows:

- i. Parameters of spatial autocorrelation modelling.
- ii. Estimation of spatial autocorrelation between samples
- iii. Block kriging estimation using mean values.
- iv. Surface estimation using Kriging (ordinary kriging, indicator kriging and universal kriging) techniques

Spatial correlation is explored using covariance function, correlograms and variogram or semivariograms.

To understand and apply the principle of geostatistics, one must understand statistical concept of random variables, means and variances.

Geostatistics compiles a set of patterns and tools established for statistical analysis of uninterrupted data. These data can be evaluated at any region in space, but are obtainable in a limited number of sampled points and value for unsampled points are estimated using geostatistics. Predictions made by Geostatistical Analysis are accompanied by information on uncertainties due to input data that are sometime polluted by errors and structure that are only approximation of the reality (Krivoruchko, 2004). The geostatistics method provides a means of interpolation based on several models.

Random Variable –geostatistics predicts the value of any property $z(x)$ where x is a point along a line, in a plane, or in 3D space, is the realization of the random variable $z(x)$. Random variable is one that takes certain probabilities.

The Mean – the mean for random variable is the expected value. The mean is calculated from (Dubrule, 2003):

$$m = E(x) = \sum_{i=1, N} X_i P_i = \int_{-\infty}^{+\infty} X f(x) dx$$

The Variance (σ^2) is the expectation of $E [(x - u)^2]$.

$$\sigma^2 = \text{Var}(X) = E\{[X - E(x)]^2\} = \sum_{i=1, N} [X_i - E(x)]^2 P_i = \int_{-\infty}^{+\infty} (X - m)^2 f(x) dx$$

The covariance defines how two random variables change together (Honerkamp, 2012). It is thus the basic tool to measure the relationship between two random variables.

The choice of the applicable interpolation method in geostatistics is determined by multiple factors. Several methods are applied to compare interpolated results or an appropriate choice may be made based on prior knowledge. For instance, if it is known that if some objects from the surface exceed the z-value it would be better to choose the Spline method. The IDW method will give a good surface when using a known z-value. IDW calculates values of grid cell locations using weights based on distances to neighboring cells. The closest point to the central one will be estimated and its weight will have greater influence in the interpolation process. IDW and Spline refer to definite interpolation methods since they are based on the neighboring measured values and the use of mathematical formulae that define the smoothness of the acquired surface.

The similarity of Kriging and IDW is that, the weights of the surrounding measured values are used for gaining prediction of un-sampled locations (Valev & Kastreva, 2010). However, in the case of kriging, it is used when there is spatial correlation or directional bias in the data.

Considering geotechnical and geological state of affairs, such as the soil strata or rock layers at a project site and drilling boreholes at some selected locations of interest, known X and Y coordinates with accurate depth recording are paramount. Many times, as anticipated, one finds that samples from boreholes closer to each other tend to be more equipotential than those from extensively distance boreholes. This observation forms the basis of the assumption in geostatistics that location has a relationship to measured properties (Hammah & Curran, 2006).

One of the fundamental practices of geostatistics has long been the prediction of the spatial structure of orebodies and the evaluation of resources and/or reserves for planning of the mining (Tolosana-delgado et al., 2015)

The relationship between the feature of interest and physical environment often is so complex that it cannot be modeled exactly (Hengl, 2009) because we only estimate a model by using the actual field measurements of the target variable.

Geostatistical methods are widely applied in spatial interpolation from point measurement to continuous surfaces (Ly et al., 2011). Geostatistics involves the analysis of the spatial dependence, creation of map processed through computer and finding probabilities that either exceed or fall below a value.

2.4 Interpolation Methods

There are several interpolation methods which include:

- (a) Inverse Distance Weighted (IDW) Method,
- (b) Triangulated Irregular Network (TIN) method,
- (c) Polygon method,
- (d) Multiquadratic Technique,
- (e) Natural Neighbor, and
- (f) Kriging

Choosing Kriging among these interpolation methods above is based on the phenomena being studied. According to Childs, C., (2004), Kriging is powerful method of interpolation used for diverse application. He also explained that kriging assumes that the distance or direction between sample points reflect a spatial correlation that can be used to explain variation in surfaces. It was further explained that kriging is the most appropriate among these interpolation methods when a spatially correlated distance or

directional bias (which can be obtained by error inherent in the instrument or caused by human error) in the data is known. It is often used for application geology and soil science.

2.4.1 Inverse Distance Weighting (IDW) Method

Inverse distance weighting models work on the premise that observations further away should have their contributions diminished according to how far away they are (Smith et al., 2015). They evaluate the relationship between interpolation accuracy and two critical parameters of IDW: power (a value), and a radius of influence (search radius) (Chen & Liu, 2012). The Inverse Distance Weighting (IDW) interpolator within the geographic information systems (GIS) operates on the assumption that entities in close proximity to one another are more alike than those farther away. IDW uses the values of surrounding measured locations to predict the value of unmeasured locations.

2.4.2 Triangulated Irregular Network (TIN) method

The TIN model represents a surface as a set of contiguous non overlapping triangles. The triangles themselves are made of sampled points as nodes. Once a surface is created by delauney triangulation, values are obtained for unsampled points on the surface.

2.4.3 Polygon method

The catchment area is divided into polygons such that each polygon has a single point of sampling (Ly et al., 2011). Each interpolated point takes the value of the closest sampled point. The advantage of this method is its simplicity. Its estimation is based on only one measurement and the information on neighboring points is ignored which is a disadvantage.

2.4.4 Multiquadratic Technique

The multiquadratic method of interpolation and prediction has attained prominence among radial basis functions because of its accuracy and simplicity. The method was named "multiquadratic" because it was originally understood, in only geometric terms, as a linear combination of quadric surfaces (Hardy, 1992).

The Multiquadratic method is considered by many to be the best in terms of its ability to fit data and produce a smooth surface (Kao & Hung, 2004). The technique minimizes the total curvature of surfaces in order to enable a variety of operations such as data visualization (Carlson & Natarajan, 1994). It has been proven that the Multiquadratic interpolation method is the best method for interpolating scattered data (Rap et al., 2009).

2.4.5 Natural Neighbor

The Natural Neighbor interpolation algorithm uses a weighted average of the neighboring observations, where the weights are proportional to the "borrowed area". The Natural Neighbor method does not extrapolate contours beyond the convex hull of the data locations, as does Thiessen polygons (Kao & Hung, 2004). However, for irregularly spaced samples and complex terrains, natural neighbor interpolations are known to perform well.

2.5 Kriging Methods of Geostatistical Interpolation

Kriging offers an optimal interpolation based on regression against observed z-values of surrounding data points. There are many kriging variants but three used in this work are, OK, IK and UK.

Kriging interpolation methods uses observations $z(x_i)$ at location x_i to estimate the values $z(x_0)$ at a point x_0 where observations are not applicable. The random variable z

at any location can be written as the sum of a deterministic component called the trend $t(x)$, and a stochastic error component, $r(x)$ (Huang et al., 2015). Assay obtained from wider-spaced drill hole can be used to calculate grade values for each block on a rectangular grid by the process of “kriging”(Everett, 2013). It gives estimates of the expected (mean) grade for each block and takes into account both nearest drill hole assays but and widely distant values. A three-dimensional “variogram” in kriging is used to estimate the variability across the distance coordinates. Variogram is used to estimate block grades. The actual grade values have a variance around the kriged values, so the kriged values will be the expected or mean for each block location, but might underestimate the variance. The variance around the kriged values is zero at the drill hole locations, and tends to increase the further a block is from a drill hole. Total grade variance is the spatial variance plus a further variance corresponding to the variability around the kriged value at each block.

2.5.1 Variography in Kriging

Kriging is built on the assumption that things that are close to one another are more alike than those that are farther apart or away, quantified as spatial correlation.

The principle of semi-variogram states that the pairs that close in distance should have smaller measurement difference than those farther away from one another.

In a semivariogram, half the difference square between the pairs of locations (the y-axis) is plotted relative to the distance that separates them (the x-axis). In creating the empirical semivariogram, the first step is to calculate the distance and squared the difference between each pair of locations. These distances can be calculated by using the Euclidean distance:

$$d_{ij} = \sqrt{(x_i - x_j)^2 + (y_i - y_j)^2}$$

The empirical semivariogram is 0.5 times the difference squared

$$0.5 * \text{average}[(\text{value at location } i - \text{value at location } j)^2]$$

2.5.2 Ordinary kriging

Ordinary Kriging is based on mathematical equation:

$$Z(S) = \mu + \epsilon(s)$$

Where; $Z(S)$ is the value at a particular location or variable of interest, μ is a constant or deterministic trend, $\epsilon(s)$ is the random error with spatial dependence or the autocorrelated error, and S represents the location.

Assuming that the $\epsilon(s)$ is intrinsically stationary, the predictor is formed as a weighted sum of the data.

$$Z(S_o) = \sum_{i=1}^N \omega_i Z(s_i)$$

Where; $Z(S)$ is the measured value at the i th location, ω_i is an unknown weight for measured value at the i th location, S_o is the prediction location, and N is the number of measured value.

Ordinary kriging uses either the semivariograms or covariance for prediction. Figure 2.1 shows the principle of ordinary kriging.

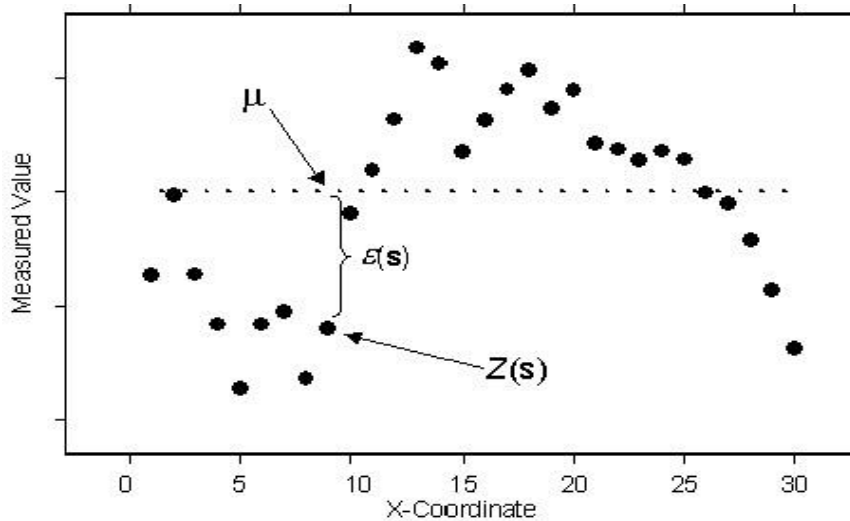


Figure 2.1: Principle of ordinary kriging

(Source: Arcgis/Arcmap 10.2.1 Manual)

Ordinary kriging along with other kriging method such as simple kriging to estimate direct solar radiation on a geographical domain characterized by orographic variability in Italy (Bezzi & Vitti, 2005). For ordinary kriging, rather than assuming that the mean is constant over the entire domain, assumed that it is constant in the local neighborhood of each estimation point (Bohling, 2005b). Given a point x_0 , the ordinary kriging estimator at x_0 based on the data $Z(x_i)$ $i = 1, \dots, N$ is defined as the linear unbiased estimator (Bonaventura et al., 2005).

Ordinary kriging is the most commonly used technique. It assumes a constant but unknown mean. Instead of weighting nearby data points by some power of their inverted distance, ordinary Kriging relies on the spatial correlation structure of the data to determine the weighting values (Ruiqing & Jin, 2012). It is widely used because it is statistically the best linear unbiased estimator (Srinivasan et al., 2008). Ordinary kriging is linear because its estimates are linear combination of the available data. It is unbiased because it attempts to keep the mean residual to be zero. Finally, it also tries to minimize the residual variance.

2.5.3 Indicator kriging

A variable that is continuous can be made into a binary (0 or 1) variable by choosing a threshold. Values above the threshold become a 1, while values below the threshold become a 0 in Geostatistical Analyst. Figure 2.2 shows the threshold of variable in space.

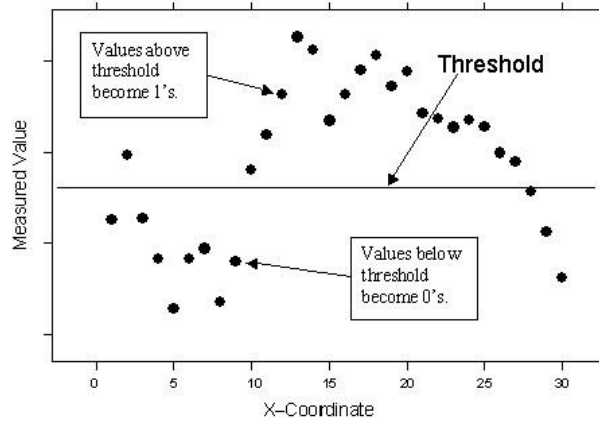


Figure 2.2: Threshold of a variable in space

(Source: Arcgis/Arcmap 10.2.1 manual) Indicator

Kriging model assumes that:

$$I(S) = \mu + \varepsilon(s)$$

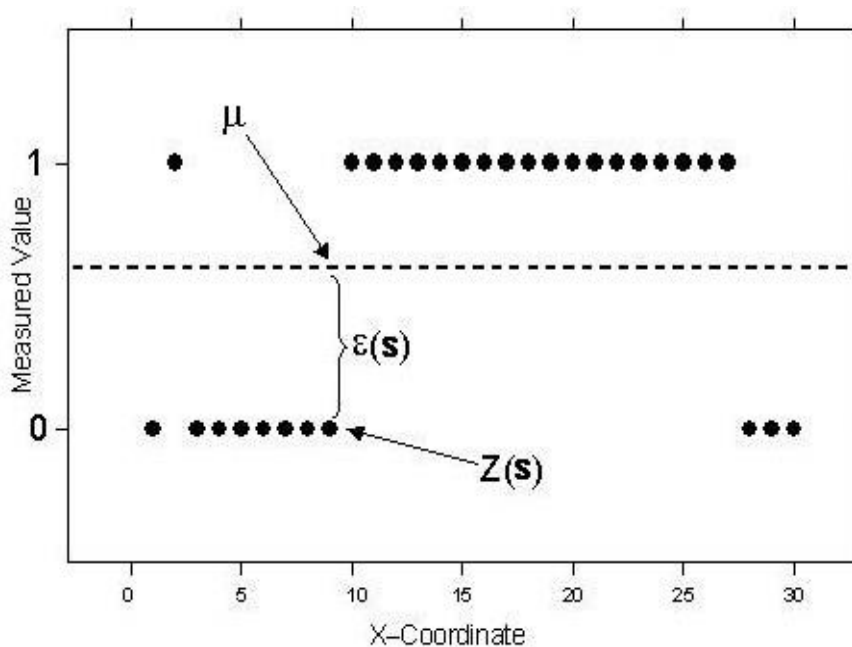


Figure 2.3: Principle of indicator kriging

(Source: Arcgis/Arcmap 10.2.1 manual)

Where μ the unknown constant, $I(S)$ is the binary value and $\epsilon(s)$ is the autocorrelated error.

Binary data is created by representing threshold as continuous data, and assumes values of 0 or 1. Indicator kriging follows as ordinary kriging using binary variable. The dashed line in the Figure 2.3 shows the unknown mean (μ) that is comparable to ordinary kriging. $\epsilon(s)$ autocorrelated in ordinary kriging, because the indicator variables are 0 or 1, indicator interpolation will be between 0 and 1.

Indicator kriging method depends on data transformation from continuous values to binary values or begins with categorical data. Probability of viral hazards from categorical data on landscape features have been produced using Indicator Kriging. It was also used on a combined variable to produce the probability map of plant disease epidemiology (Tolosana-Delgado et al., 2008). Indicator kriging (IK) has been used to categorize several lithological units of an iron ore deposit (Kameshwara Rao &

Narayana, 2015) as well as to estimate the pollution in waterways associated with agricultural use (Lyon et al., 2006), and also to generate coastal sediment type map (Fu-cheng et al., 2012)

2.4.3 Universal kriging (UK)

Universal Kriging assumes model:

$$Z(s) = \mu(s) + \varepsilon(s),$$

Where; $\mu(s)$ is some deterministic function. The principle of universal kriging is shown in figure 2.4.

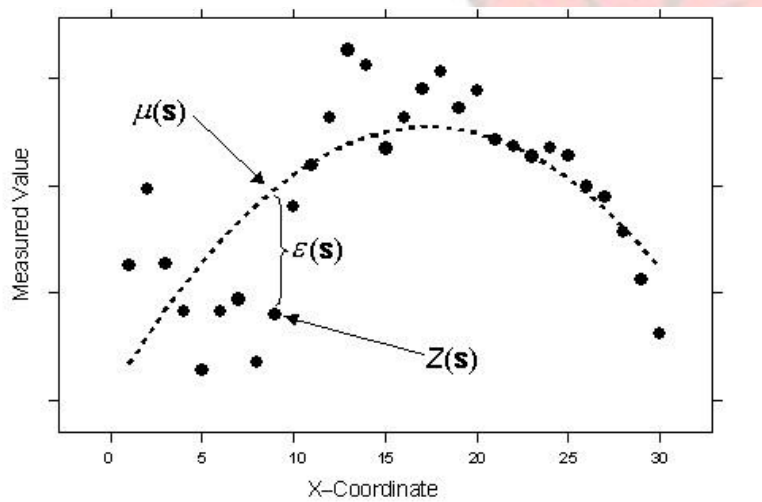


Figure 2.4: Principle of Universal Kriging

(source: Arcgis/Arcmap 10.2.1 Manual)

A second-order polynomial is the trend which is $\mu(s)$ and when subtracted from the original data, results in the errors, $\varepsilon(s)$, which are assumed to be random. The average of all $\varepsilon(s)$ is 0. The random errors $\varepsilon(s)$ are used to model the autocorrelation. Universal kriging is similar to regression with the spatial coordinates as the explanatory variables. The errors are modeled to be autocorrelated assuming they are independent.

The United States army used Universal kriging for closely monitoring the changing depths of navigation channels throughout the U. S. A. and Western Europe. The method uses local or global polynomial functions to detrend data (Sterling, 2003). Investigation of the practical and methodological use of universal kriging of functional data to predict unconventional shale production in undrilled locations from known production data was conducted using two estimation procedures, using estimation by means of cokriging of functional components (Universal Cokriging, UCok), requiring cross-variography and estimation by means of trace-variography (Universal Trace-Kriging, UTrK), which avoids cross- variogram modeling (Menafoglio et al., 2016). Universal Kriging has also been used to interpolate water table elevation from their measurement at random locations in New Mexico, USA. In this instance, Statistical analysis performed on the estimated contours revealed that the decrease in water table was between 0.6 and 4.5 m at 90% confidence(Kambhammettu et al., 2011). In the case where there is considerable correlation between analyzed variable and certain other spatial variable such as altitude, east-west coordinate or others, universal kriging is preferred (Agency, 2010).

Universal kriging is mostly used when trend is present. A nonstationary regionalized variable is composed of drift, or the expected value of the variable in a neighborhood, and the residual which is the difference between the drift and the actual value (Grant, 1990). It was proven that universal kriging based on a universal method of variogram estimation is more flexible and more intuitive than kriging of intrinsic random functions(Boogaart & Brenning, 2001). Universal Kriging matrix (M), which includes in it the values of the polynomials at data locations (matrix F), in some cases may have a too large condition number and can even be nearly singular due to the fact that some columns are close to be linearly dependent(Lopez & Samper, 2007). Universal kriging

was applied to the command area of a set of canal irrigation projects in north- western India to show its applicability for optimal contour mapping of groundwater levels(Kumar, 2007). Universal kriging incorporates trend estimation error as well as spatial interpolation error minimized to produce quality maps by the interpolation of observation of a target environmental variable at a restricted number of locations(Brus & Heuvelink, 2007). Using a spherical variogram model on the basis of crossvalidation, the universal kriging results were comparable with the subjectively obtained map (Kastelec & Košmelj, 2002).

2.6 Geographic Information Systems (GIS)

Geographic Information Systems (GIS) is a Geographic Information Systems system of software, hardware and efficient data that facilitates the enhancement, modeling, development and display capabilities and enables the user to analyze and interpret the data. Configured properly, GIS can model features or existences as a function of the other features or phenomena that may be interrelated where all features are categorized by spatial and attribute data.

Integrated methodology using various Kriging methods such as OK, IK and UK in GIS was used to display the possibility of using these methods in mapping the spatial distribution of iron, silica and alumina content in the iron ore deposits of the mount Tokaden, in Liberia. GIS software (ArcGis 10.2.1) was used to post the location and geological map of the study area.

This integrated method simplified the determination of the mining production parameter as well as mapping out at any time the current status of the mining area in terms of ore thickness, silica content, and alumina content, over burden and other metal content within the ore deposit.

Dynamic software and strong databases are needed to improve update, implement, and always give a true picture of circumstances on the ground.

CHAPTER THREE

MATERIALS AND METHODS

3.1 The Study Area

Liberia has about 43,000 square miles (11137.011 km²) of land area and lies between latitude 9°33'N and 3°31'N and longitude 11°18'W and 7°17'W. It is bordered on the North by the Republic of Guinea, west by the Republic of Sierra Leone, East by the Republic of Cote D'Ivoire, and South by the Atlantic Ocean (Hadden, 2006).

The Tokadeh region of Nimba County lies between latitude 7°15'N and 7°45'N and longitude 8°15'W and 8°45'W. Figure 3.1 shows the map of the study area.

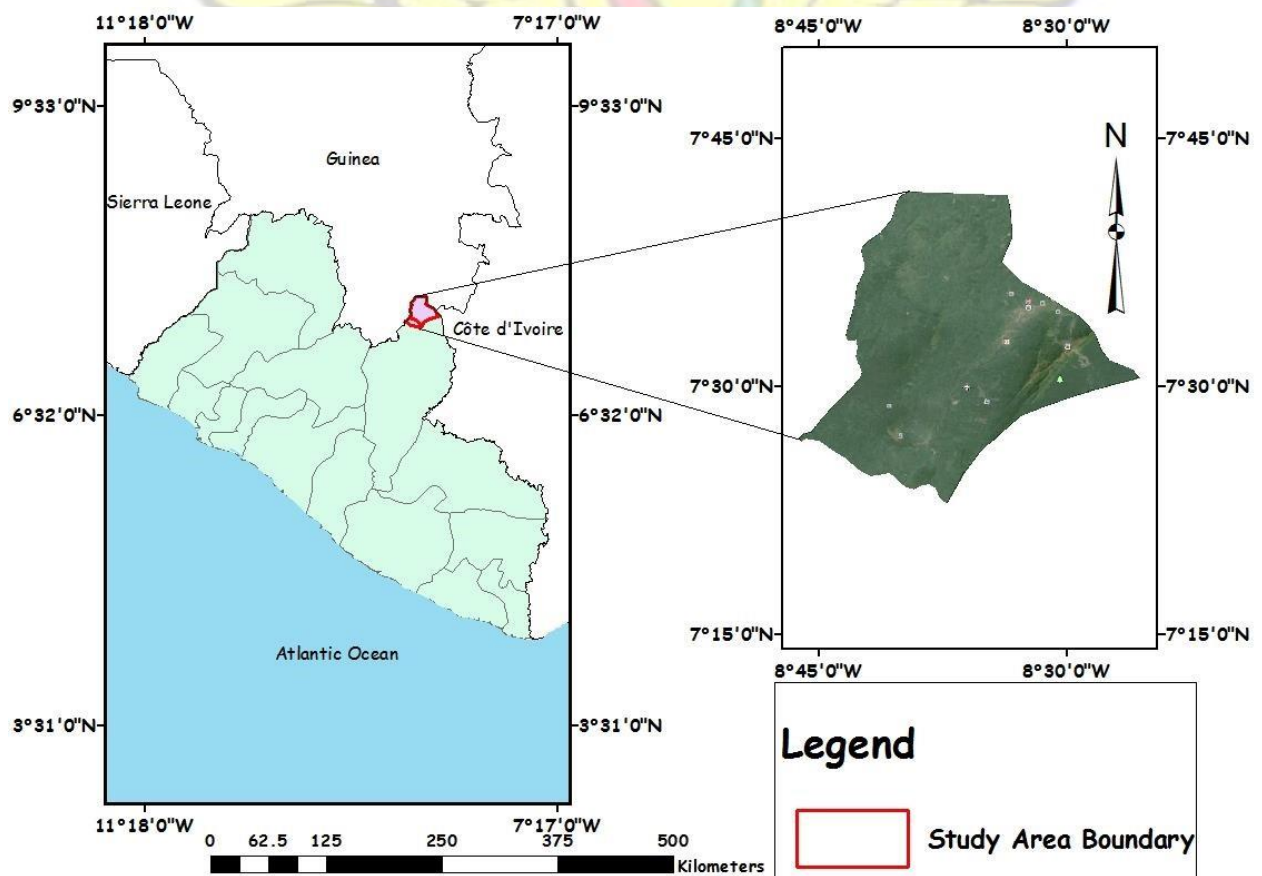


Figure 3.1: Map of Tokadeh (Study Area)



Figure 3.2: Google earth image of Tokadeh Mining Site

3.1.1 Geology

Liberia is perched on the West African Shield, a rock formation from 2.7 to 3.4 billion years old, which is made of granite, schist, and gneiss. This shield has been intensely folded and faulted and is interspersed with iron-bearing formations known as itabirites in Liberia.

Nimba County lies between latitude 7°45'N and 5°45'N and longitude 9°15'W and 8°15'W with the population of 462,026 (Liberty, 2008). It has a tropical climate with alternating wet and dry seasons. Annual rainfall is as little as 200 cm. Temperatures are moderate all year in the highest parts of the county. Rain forest dominates except for a few savannahs at higher altitudes, most of which have formed on iron-formation pebble conglomerate (canga). The county seat of government is Sanniquellie. Much of the

population is dispersed in small tribal villages with high farming activities mainly in rubber, coffee, cocoa, palm, rice, cassava, plantain and other vegetables.

Valuable iron ore reserves are found primarily in four areas: the Bomi Hills (Bomi county), the Bong Range (Bong county), the Mano Hills (Grand Cape Mount County), and Mount Nimba (Nimba county), where the largest deposits occur. Other minerals such as diamonds, gold, lead, manganese, graphite, cyanite, and barite are also found in these areas (Hadden, 2006). The Mt. Tokadeh region, study area, has large known ore deposits. Currently a concession has been given to ArcelorMittal

Liberia. The deposit at Tokadeh is situated in the Western Area of the Mt. Nimba Range. This deposit is in part of Mount Nimba strands Liberia, Guinea, and the Cote D'Ivoire.

The iron deposit at Tokadeh is associated with schist and gneiss of probable sedimentary origin of the Archean age Iron formation, resting predominantly gneissic basement complex. The metamorphic grade increases from lower epidote-amphibolite faces to amphibolite lower-granulite faces in the Tokadeh ridge (Yves Buro, 2009)

Four (4) horizons of iron formations separated by schist-gneiss bands were recognized from drilling and mapping by LAMCO. Two (2) Iron Formations separated by one schist- gneiss unit were interpreted by Met-Chem from the deeper boreholes. The three (3) bands of interfingering schist-gneiss predominantly found in the western portion of Tokadeh appear to grade in a single unit toward the east.(Yves Buro, 2009)

The iron formation is mainly a metamorphosed, oxide-type banded iron formation made up of an assemblage of quartz and magnetite, with ubiquitous, locally abundant iron silicates (amphibole, pyroxene). The Tokadeh basement gneiss is described by LAMCO as a medium-grained, light grey but generally reddish potassic rock. The gneiss between

the iron formations is a light- grey, medium-grained quartz-feldspar rock, with occasional amphibole-rich zones. The basement gneiss and the upper gneiss were found by Met-Chem to include both potassic (granitic) or more mafic (grano-dioritic) varieties. (Yves Buro, 2009).

3.1.2 Climate

Liberia is known for its sustained heat and heavy rainfall, its climate is tropical and humid, with little changes in temperature throughout the year. The log mean temperature is 27°C (81°F), with temperature exceeding 36°C (97°F) or falling below 20°C (68°F). The annual temperature in the region is 24.4°C, with a minimum of 10.8°C in January and a maximum of 34.7°C and 34.4°C in the month of February and March. The Yekepa area has a sub-equatorial climate subject to the southwesterly monsoon from the ocean and the north end dry north-easterly harmattan winds from the desert. Average annual precipitation is recorded at about 1,750 mm between April and October with a peak in September with about 3,000 mm rainfall at the highest altitudes.

3.1.3 Local Population

There is no village in the operational area of Mt. Tokadeh, however, there are several little villages that consist of tens of thousands inhabitants who are mostly farmers scattered around the project area. The Major crops grown in this area are rubber, coffee and cocoa for commercial purpose and rice, cassava, plantain and other vegetables mainly for consumption.

3.2 Materials

3.2.1 Sampled Data

ArcelorMittal Liberia Limited provided the facilities and equipment used to drill 110 boreholes. The X and Y coordinates as well as ore thickness in each ore zone and the

Z coordinates were recorded.

Diamond drill rig equipped with line wire system to retrieve samples while drilling was used to drill through the earth at varying depths. The minimum and maximum drill hole depth was 21.35m and 550.55m correspondingly. Cylindrical core samples were collected at 1m and 2m respectively due to the layout of the land surface. Samples collected were placed in long plastic sack marked with drill-hole sample ID.

The physical properties of these samples such as rock type, core recovery, hardness, color, weathering, structure data, mineralogical assemblage, grain size, and texture profile were tested at the ArcelorMittal laboratory equipped to testing soil sample for minerals.

The drill holes were branded one after the other and locations coordinates were measured in Universal Transverse Mercator (UTM) system, while all distances were measured in metre. The Azimuth, angle showing reference direction (North) and line from the observer to a point of interest projected on the sample plane.

The interval of each ore zone, i.e., oxide ore, transition ore, and primary ore were identified and recorded for each drill hole. Table 3.1 shows 20 samples out of the 110 samples collected, while Table 3.2 gives a summary of data extracted.

Table 3.1: Drill hole data

Drill Hole ID	Coordinate (UTM)			Dip, °	Azimuth, °	Total depth	Oxide ore			Transition ore			Primary ore		
	X	Y	Z				From (m)	To (m)	Interval (m)	From (m)	To (m)	Interval (m)	From (m)	To (m)	Interval (m)
T502	536479.9	823949.6	712.927	-90	0	238.75	0	74.5	74.5	74.5	118.8	44.3	118.8	238.75	119.95
T504	536099.2	824153.6	690.588	-90	0	243.1	0	15.3	15.3	15.3	27	11.7	27	202.7	175.7
T505	536810.5	825582.3	660.576	-90	0	300.4	0	58	58	58	85.1	27.1	85.1	243.1	158
T506	536635.3	824334.9	612.018	-90	0	300.15	0	27.48	27.48	15.3	27.48	37.05	37.05	300.15	263.1
T507	536879.7	823903.4	593.25	-90	0	475.45	0	37	37	37	47	10	47	475.45	428.45
T508	536999.7	824162.4	561.189	-90	0	193.9	0	10	10	10	30	20	30	193.9	163.9
T509	536276.6	824466.8	654.955	-90	0	287.65	0	29.55	29.55	29.55	33	3.45	33	287.65	254.65
T510	536458.4	824870.6	653.218	-90	0	300.25	0	24.55	24.55	24.55	56.25	31.7	56.25	300.25	244
T511	535468.6	824019.2	826.722	-90	0	87.85	0	22.55	22.55	22.55	41.6	19.05	41.6	87.85	46.25
T512	535749.5	824345	764.897	-90	0	248.5	0	10.2	10.2	10.2	28.24	18.04	28.24	248.5	220.26
T513	535563.1	824429.7	825.089	-60	297	302.4	0	69.24	69.24	69.24	89.3	20.06	89.3	302.4	213.1
T514	535923.3	824702.5	743.597	-90	0	306.9	0	59.75	59.75	59.75	69.75	10	69.75	306.9	237.15
T515	535833.3	824740.3	757.33	-90	0	206.25	0	17.8	17.8	17.8	19.8	2	19.8	206.25	186.45
T516	536633.1	825247.6	679.835	-90	0	322.5	0	28.02	28.02	28.02	46.94	18.92	46.94	322.5	275.56
T517	536999.1	825064.6	616.66	-90	0	343.6	0	45.4	45.4	45.4	51.17	5.77	51.17	343.6	292.43
T519	536725.4	825410	669.266	-90	0	59.75	0	22.6	22.6	22.6	24.44	1.84	24.44	59.75	35.31
T520	536407.4	825128.5	704.545	-90	0	274.95	0	52.6	52.6	52.6	95.4	42.8	95.4	274.95	179.55
T521	536818.2	824696	576.653	-90	0	50.15	0	5.03	5.03	5.03	17.62	12.59	17.62	50.15	32.53
T522	537353	823989.9	530.336	-90	0	288.65	0	21.8	21.8	21.8	36.83	15.03	36.83	288.65	251.82
T523	537186	824520.4	551.725	-90	0	442.25	0	10.5	10.5	10.5	22.32	11.82	22.32	442.25	419.93

Table 3.2: Summary of Data Extracted from drill hole database use in model for interpolation

Collar	Drill hole ID, UTM_X, UTM_Y, Z (Total Depth)
Assay	Drill hole ID, From(m), To(m), Interval, Fe%, Fe2O3%, Al2O3%, SiO2%, CaO%, Mgo%, K2O%, Na2O, Mno%, TiO2%, Cr2O3%, P2O5%,Lol%, S%, Davis tube, Satmag%
Oxidation	Drill Hole ID, From(m), To(m), Interval(m)

(Source: Author's construct)

3.2.2 Other Materials

Software used for processing includes ArcGIS, Voxler, Microsoft Excel and

Microsoft Word used for report compilation

3.3 Methodology

The coordinate of the drill site were verified for integrity by using RTK GPS on some randomly selected bore holes. The integrity of the drill holes data were protected by the team at various stages. These data were entered by logging geologists into excel templates, and was checked by peer review team on the field. The collars for all the holes were picked using differential GPS or Total Station (RTK). Errors were checked by comparing the results with the fix from the hand-held GPS over the casing of the borehole. Data in excel template from drill hole were exported into a shapefile format and inputted into Arcgis/Arcmap 10.2.1 for interpolation using various kriging interpolation techniques (ordinary kriging, indicator kriging and universal kriging).

These three interpolation methods (ordinary, indicator, and universal) in kriging were used to analyze and predict grade and concentration at unsampled locations at Mt. Tokadeh mining site. Creative colours were used in these three kriging interpolation techniques to delineate the relative quality of ore at various locations. To better appreciate the colour combinations that delineate various types of minerals within the mining site, four classes of colour were used for delineation. To better distinguish the quality of prediction, the four curves were drawn; predicted curve, error curve, standard error curve, and normal QQPlot curve. The detailed methodology is shown in Figure

3.3

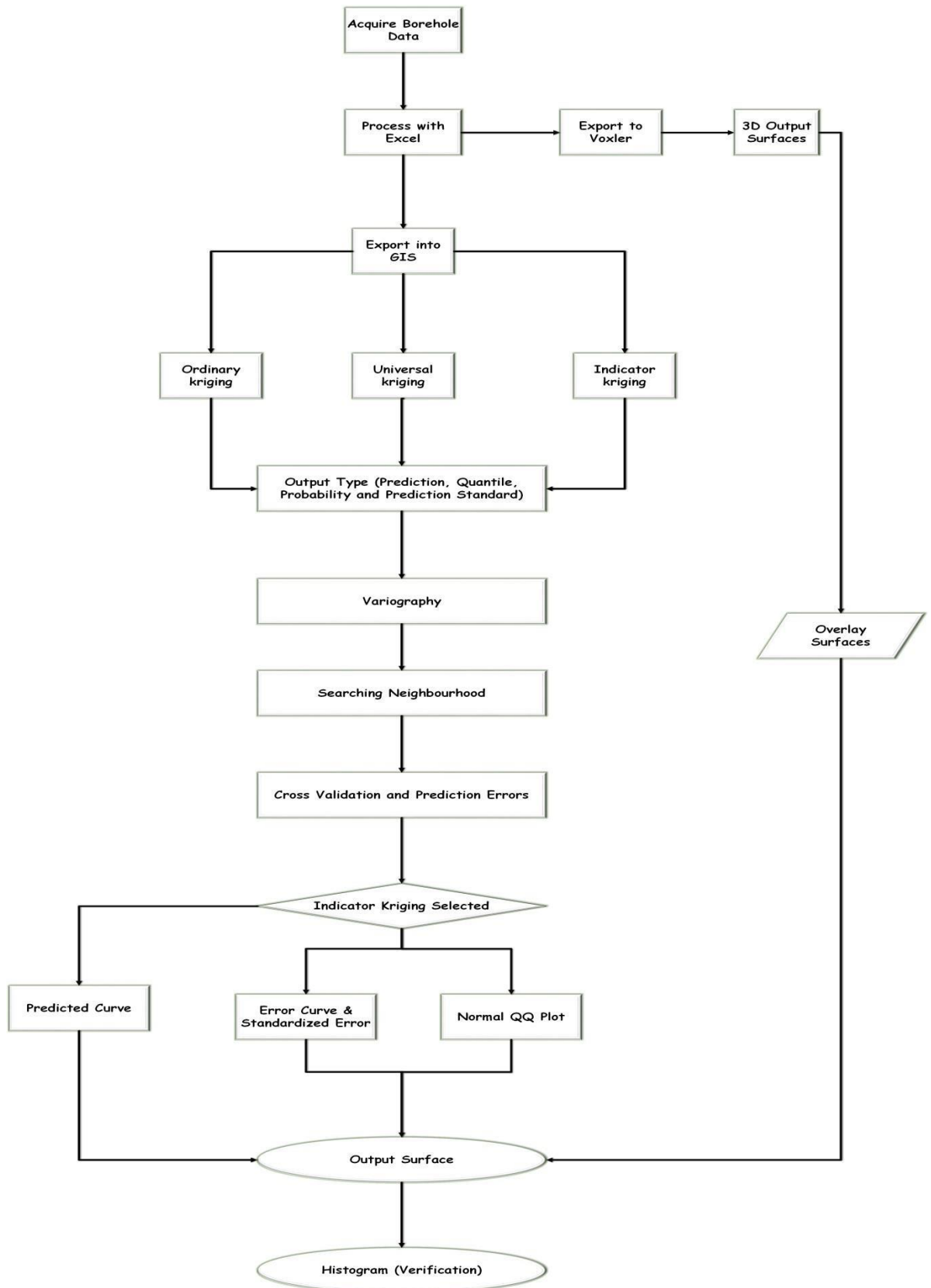


Figure 3.3: Design of work flow

3.3.1 Geostatistical data analysis

Various types of kriging (OK, IK, and UK) were used and the one that best suit this interpolation was selected and used base on careful analysis of their result. Results of each interpolation are presented, compared and results were analyzed in chapter 4 to select the best kriging method for this work.

The processes in the kriging were outline in following steps:

Steps 1 and 2: Selection of the kriging type. (Indicator, universal, ordinary)

By default, Ordinary (kriging) and Prediction (map) are selected in the dialog box. However, it is required to visualize which method gave the best results. These default values are changed appropriately.

Step 3: Semivariogram/Covariance modelling (Variography)

The semivariogram/covariance model is displayed, allowing one to examine spatial relationships between measured points. It allowed one to explore and select the best fitting semivariogram model that captured the spatial relationship in the data.

Step 4: Searching Neighborhood

The crosshairs showed a location that had no measured value. To predict a value at the crosshairs, the values at the measured locations are used. Using the surrounding points and the semivariogram/covariance model fitted previously, values were then predicted for the unmeasured locations. (Figure 3.4)

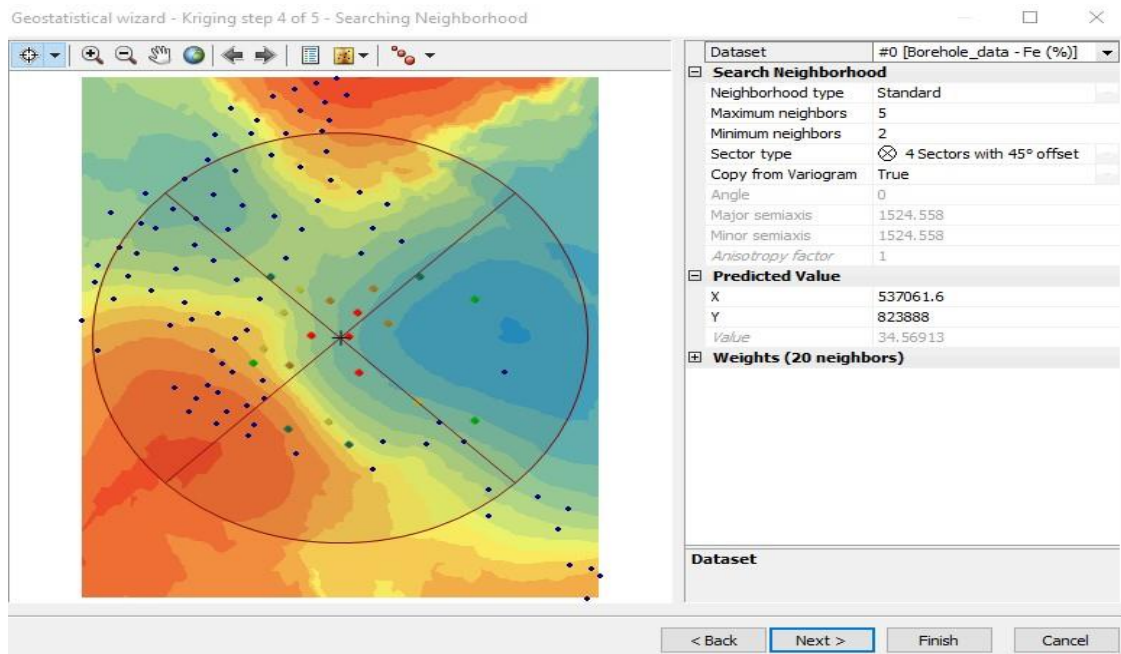


Figure 3.4: Searching neighborhood

Step 5: Cross validation

The cross-validation diagram gives one an idea of how well the model predicts the values at the unknown locations. It is used to assess how accurate the selected interpolation model is. Using Cross validation, a point is taken out of the dataset leaving the remaining point within the dataset and uses the rest to predict that location. The point taken out is then replaced to the dataset and different point is taken out. This procedure is implemented on all the points within the dataset to provide pairs of prediction and known values that feasibly compared to exploit model's performance. The results of these procedures are then summarized as a means and root mean square error. In the cross validation, the various curves are displayed for prediction analysis. These curves are, error curve, standard error curve, predicted curve, and the normal quantile-quantile (QQ) plot curve.

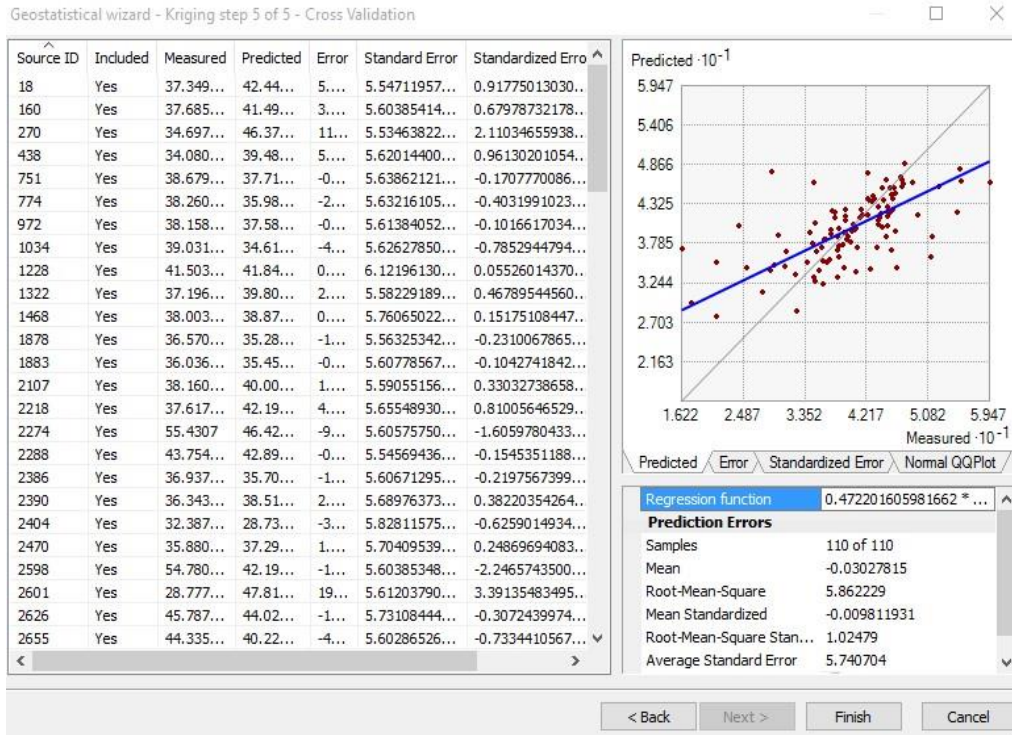


Figure 3.5: Cross validation

By default, the Method Report dialog box (Figure 3.6) summarizes the results and it associated parameters that are used to actualize the output surface map.

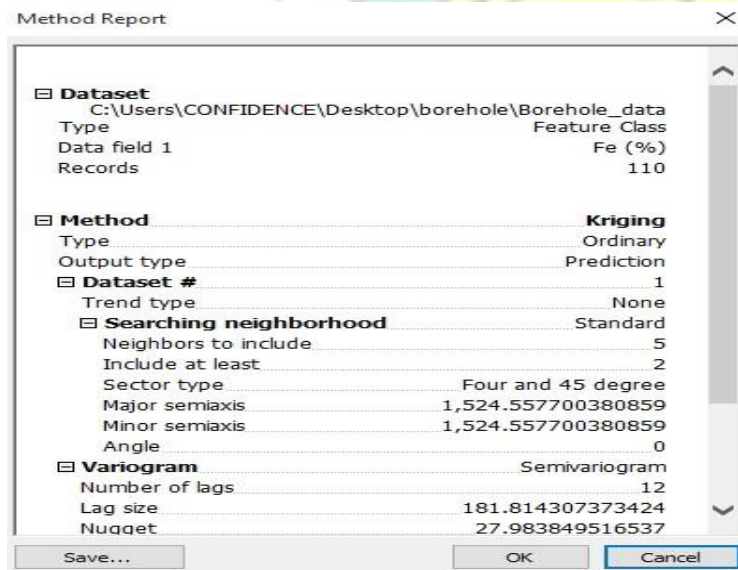


Figure 3.6: Method Report

The final output maps are shown as either Prediction map or other output maps within the model in chapter 4. Three interpolation surfaces were drawn to allow the user analyze the data in variety of ways. The three interpolation surfaces are as follow:

- a. Prediction map; produced from interpolation values (Figures 4.6, 4.7 and 4.8)
- b. Probability map specifies threshold and produces probabilities map which allow one to know the predicted values exceed or do not exceed the specific threshold (Figures 4.9, 4.10 and 4.11)
- c. The Error of Prediction map is produced from standard error interpolated values. It is also called standard error of interpolated indicator values (Figures 4.12, 4.13 and 4.14)

3.3.2 Voxler

Voxler is a three-dimensional scientific visualization program primarily used for volumetric rendering and three-dimensional data display and analysis. Voxler was used to generate a 3D rendering of the bore hole data. The result was overlaid on the final kriged map to validate the prediction made whether or not they are in conformity with the drilled data. It also possesses built-in computational modules such as threedimensional resampling, image processing gridding, and numerous lattice operations. It is designed for displaying XYZC data, where C is a variable at each X, Y, and Z location.

CHAPTER 4

RESULTS AND ANALYSIS

4.1 Results

The results of the kriging in Tables 4.1, 4.2, and 4.3 show that the indicator kriging which uses the threshold, was the best suited for this work. These values are obtained from the variogram modeling as a first step in Figures 4.1, 4.2 and 4.3. The exponential empirical model was found to be the best because this removes the nugget effect from the data. The semivariogram of all the three interpolation surfaces in kriging (OK, IK, and UK) proved that the iron content was normally distributed within the study site. The binned, or point in the red in the semivariogram below were grouped by default based on their distances from one another and the average distance for each bin were plotted.

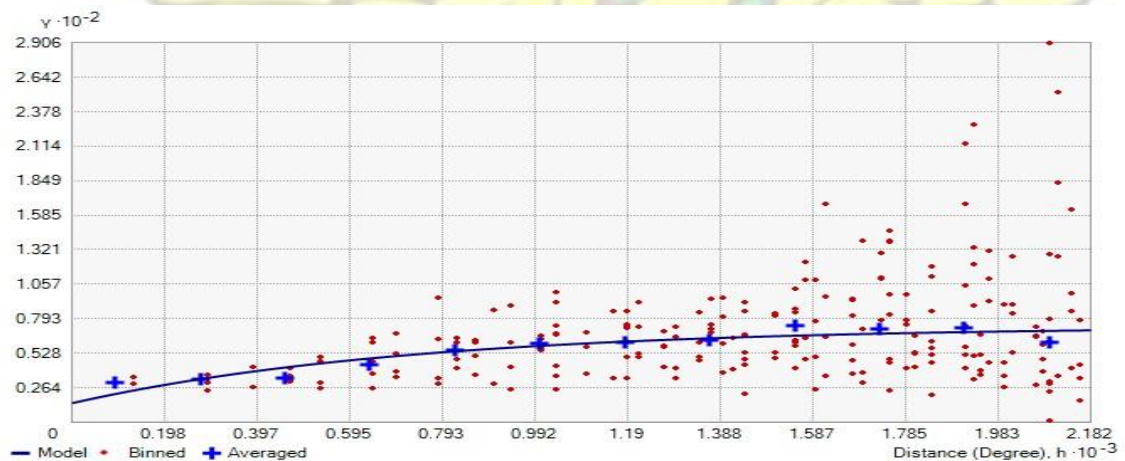


Figure 4.1: Semivariogram of Iron (Fe) distribution (OK)

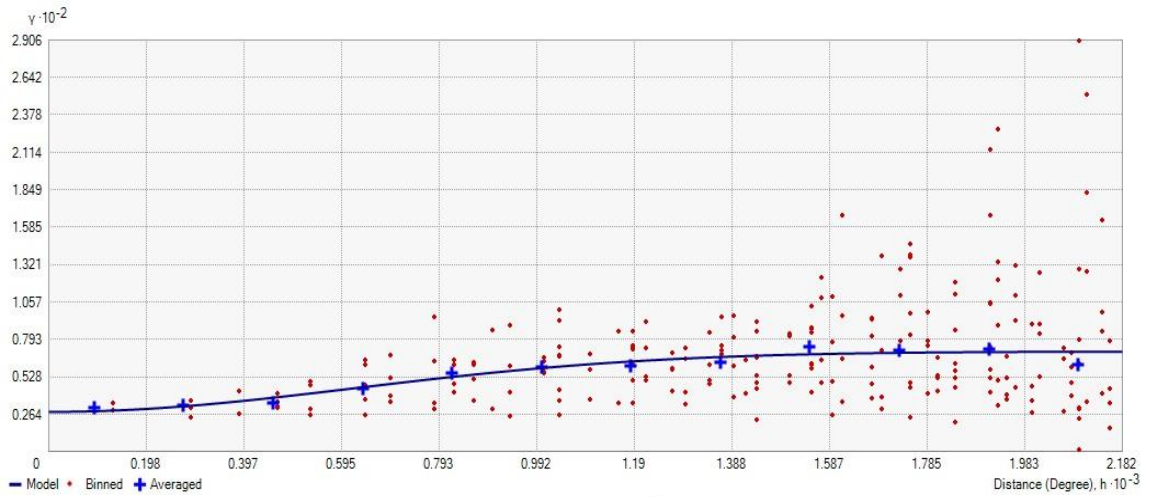


Figure 4.2: Semivariogram of Iron (Fe) distribution (UK)

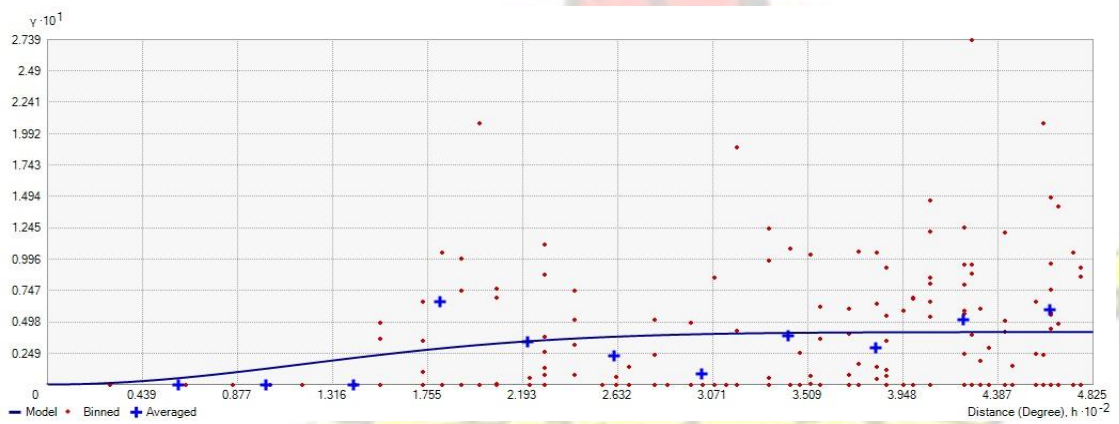


Figure 4.3: Semivariogram of Iron (Fe) distribution (IK)

Secondly, the histogram which examines the distribution and summarized statistics of the dataset prove also that iron (Fe) content using the three interpolations were all normally distributed. Analyzing statistics provided by histogram for all three interpolations, the mean (39.921) and median (40.294) were all similar, the skewness were all near zero and the kurtosis was near 3. Below are the general statistical results of the various histograms. Table 4.1 summarizes the statistical analysis result of Iron, Silica and Alumina gain from the total of 5444 samples from 110 bore holes and Figure 4.4 showing the histogram analysis.

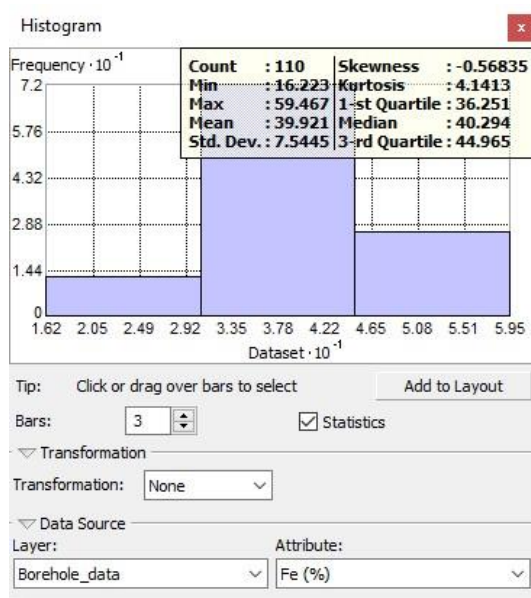


Figure 4.4: Histogram showing statistical result of iron (Fe) distribution in kriging

Table 4.1: Statistical concentration analysis result of Iron, Silica and Alumina

Statistical concentration analysis of 5444 samples from 110 bore holes					
Iron	Silica		Alumina		
Number of Samples	Concentration (%)	Number of Samples	Concentration (%)	Number of Samples	Concentration (%)
267	0.72-13.93	429	0.02-18.34	5228	0.015-15.15
186	13.93-27.13	1027	18.34-6.65	194	15.15-30.29
2791	27.13-40.34	3732	36.65-54.97	9	30.29-45.43
1912	40.34-53.55	233	54.97-73.28	6	45.43-60.56
288	53.55-66.76	23	73.28-91.60	7	60.56-75.7

(Source: Author's construct)

Selection of the best among the three interpolation techniques depends on the cross validation process. The result summarized as means and root mean square errors are compared. The interpolation with the closest predicted value and least average standard error is considered the best.

Cross validation result shows that OK Table 4.1 and UK Table 4.2 predicted values were too far from the measured values, with average standard error of ± 5.7 as compared

to IK whose predicted values were close to the measured value and with an average standard error of ± 0.2 . IK also gave the opportunity of setting a threshold unlike OK and UK which interpolated using deterministic means.

Table 4.2: Prediction Errors OK Kriged result

Prediction Errors OK	
Samples	110 of 110
Mean	-0.0303
Root-Mean-Square	5.8622
Mean Standardized	-0.0098
Root-Mean-Square Standardized	1.0248
Average Standard Error	5.7407

(Source: Author's construct)

Table 4.3: Prediction Error IK Kriged result

Prediction Errors IK	
Samples	110 of 110
Mean	-0.0066
Root-Mean-Square	0.2537
Mean Standardized	0.0008
Root-Mean-Square Standardized	1.3065
Average Standard Error	0.1755

Table 4.4: Prediction Error UK Kriged result

Prediction Errors UK	
Samples	110 of 110
Mean	-0.03027815
Root-Mean-Square	5.862229
Mean Standardized	-0.009811931
Root-Mean-Square Standardized	1.02479
Average Standard Error	5.740704

(Source: Author's construct)

The IK posted Mean Prediction Error and the Mean Standardized Prediction Error of (-0.0065 and 0.0008) respectively which are close to zero indicating that the prediction values were unbiased. The Root-Mean-Square (1.3064) prediction error is very close to one, which also showed that it is a suitable and best fit between the point estimates of Fe%. But the Average Standard Error of OK and UK (± 5.7) and RootMean-Square prediction error (± 5.8) were nearly similar, showing that these models overestimated the variability of Fe% as compared to IK which was ± 0.2 . The average standard error display by OK and UK proved that these models were unsuitable for this dataset.

Finally, the normal QQPlot curve (Figure 4.5) showed the Fe distribution trend

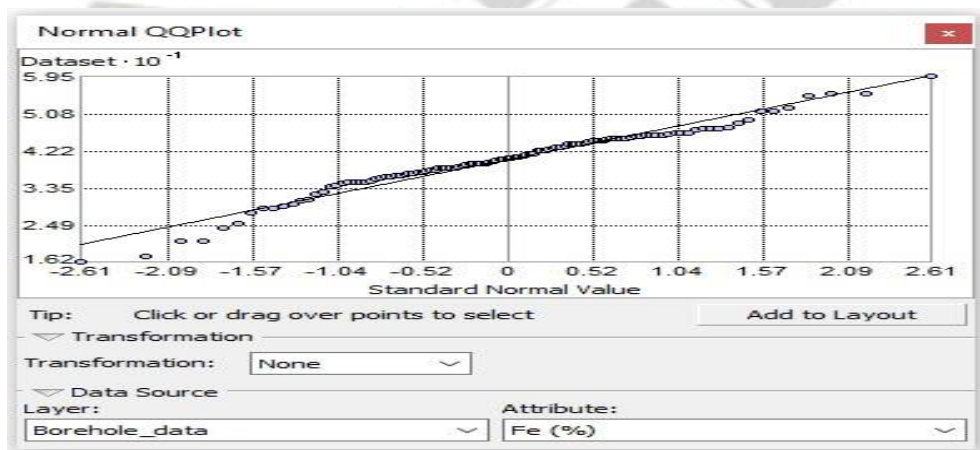


Figure 4.5: Normal QQPlot

These points along the 45 degree line show that the Fe% was slightly normally distributed.

Output maps

Figures 4.6, 4.7 and 4.8 show the output prediction map from the interpolation of the three kriging techniques (OK, IK and UK) used in this work. An examination of the three maps show that the OK and UK kriged maps show a concentrated iron region in

the northern and south western corner which do not truly represent the clear concentration as compared to IK kriged map which shows conformity with field data.

Validating IK Kriged map, twenty samples data were randomly selected and reserved. These data were processed and overlaid on the IK Kriged output map (Figure 4.7) which validates the conformity of the output map. Areas with high Fe concentrations from the reserved result confirmed locations of high concentration of Fe in areas of the IK Kriged map after an overlay was performed. Validation was also performed to further verify IK Kriged result using the 3D output projected from Voxler (Figure 4.17). These 3D Voxler results also confirmed with IK Kriged results when overlaid.

Finally, the Silica and Alumina distribution maps (Figures 4.15 and 4.16) were overlaid on the Fe distribution map to validate the areas of concentrations of both impurities. The blue colours on the Alumina and Silica distribution maps signified low concentration in Silica and Alumina whereas the red colour signified high concentration in Silica and Alumina. Similarly, areas that show blue on the Fe distribution map signifies low Fe content, and the colour red signified high Fe content. These results proved that areas that show low content of impurities, the Fe content is high and areas that show high content of impurities, the Fe content is low (Amikiya, 2014).

Figure 4.7 is an IK kriged map at 25% threshold. This result shows that there are commercial quantities of Fe within the study area. The color delineation shows northern and southern portion in red, which indicate 25% of Fe concentration in these locations, thus making the study area commercially viable, while the central region of the map shows high concentration of Alumina and Silica content.

To further delineate the Fe concentration at the study area, threshold was set at 40% in Figure 4.10. The result shows a high Fe contraction at the northern, south western and

south eastern corners of the map shown in red, making these areas highly concentrated with iron ore and considered as DSO. If processed, the quality of these areas will improve up to 65% Fe concentration.

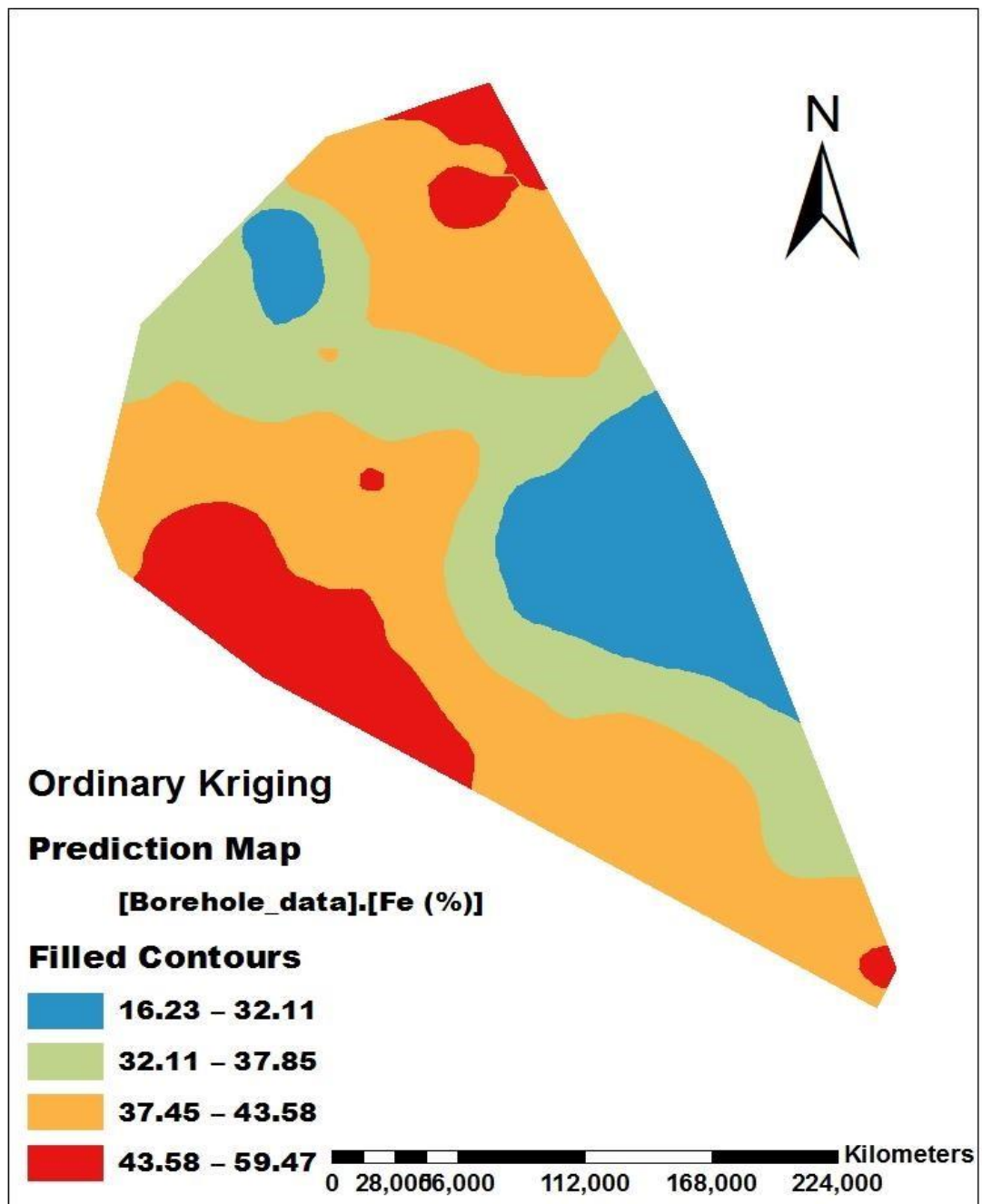


Figure 4.6: Ordinary Kriged Prediction

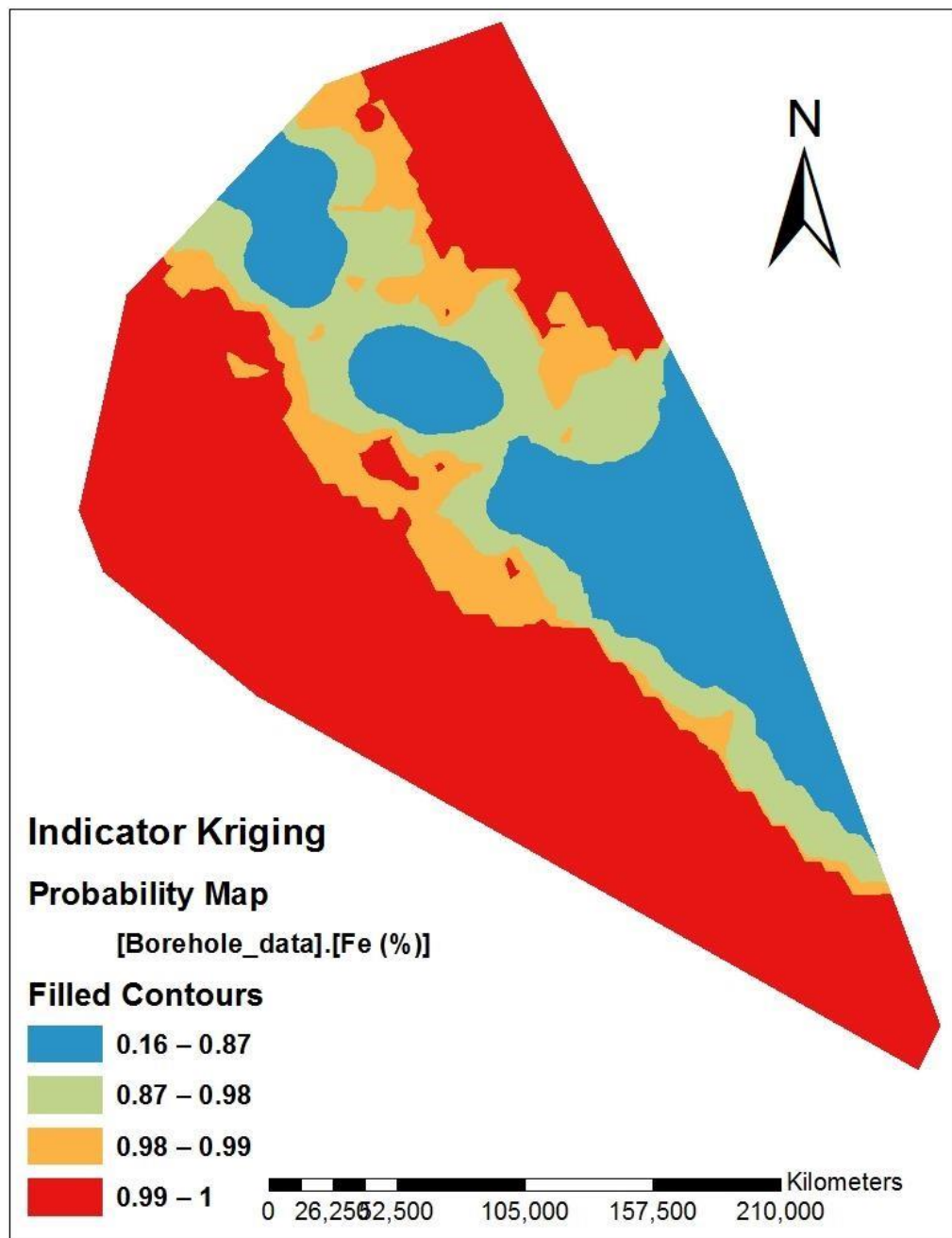


Figure 4.7: Indicator Kriged Prediction

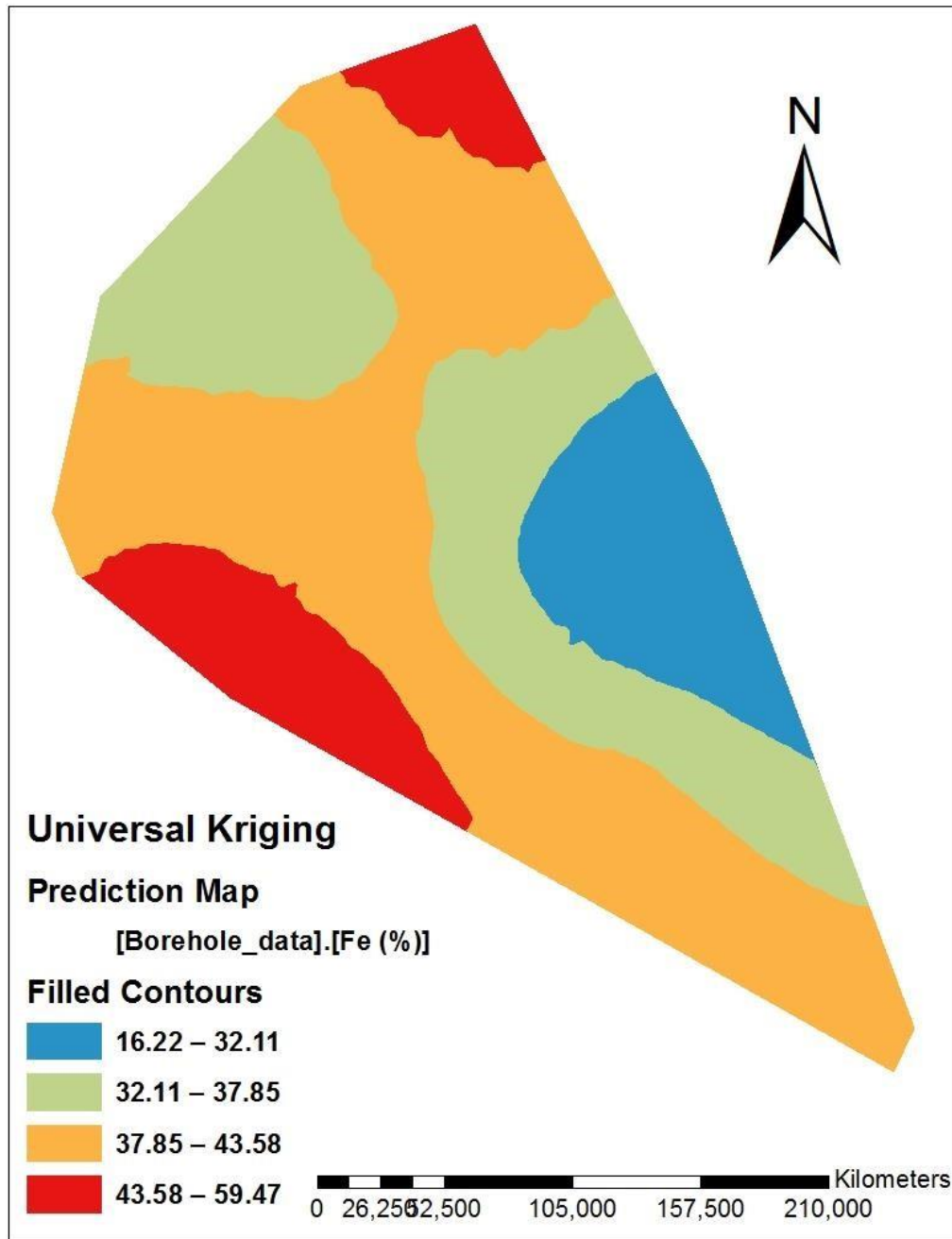


Figure 4.8: Universal Kriged Prediction Map

These probability maps shown in Figures 4.9, 4.10 and 4.11 proved from visual analysis that IK prediction map (Figure 4.10) predicts well because it shows the mineral distribution and specified concentrated area within the study area as compared to OK kriged and UK kriged probability maps using 40% threshold for all the interpolation

techniques. Figures 4.12, 4.13 and 4.14, show the standard error map. From visual analysis, the IK kriged standard error map (Figure 4.13) shows more normal distribution as compare to OK kriged and UK kriged standard error maps.

KNUST



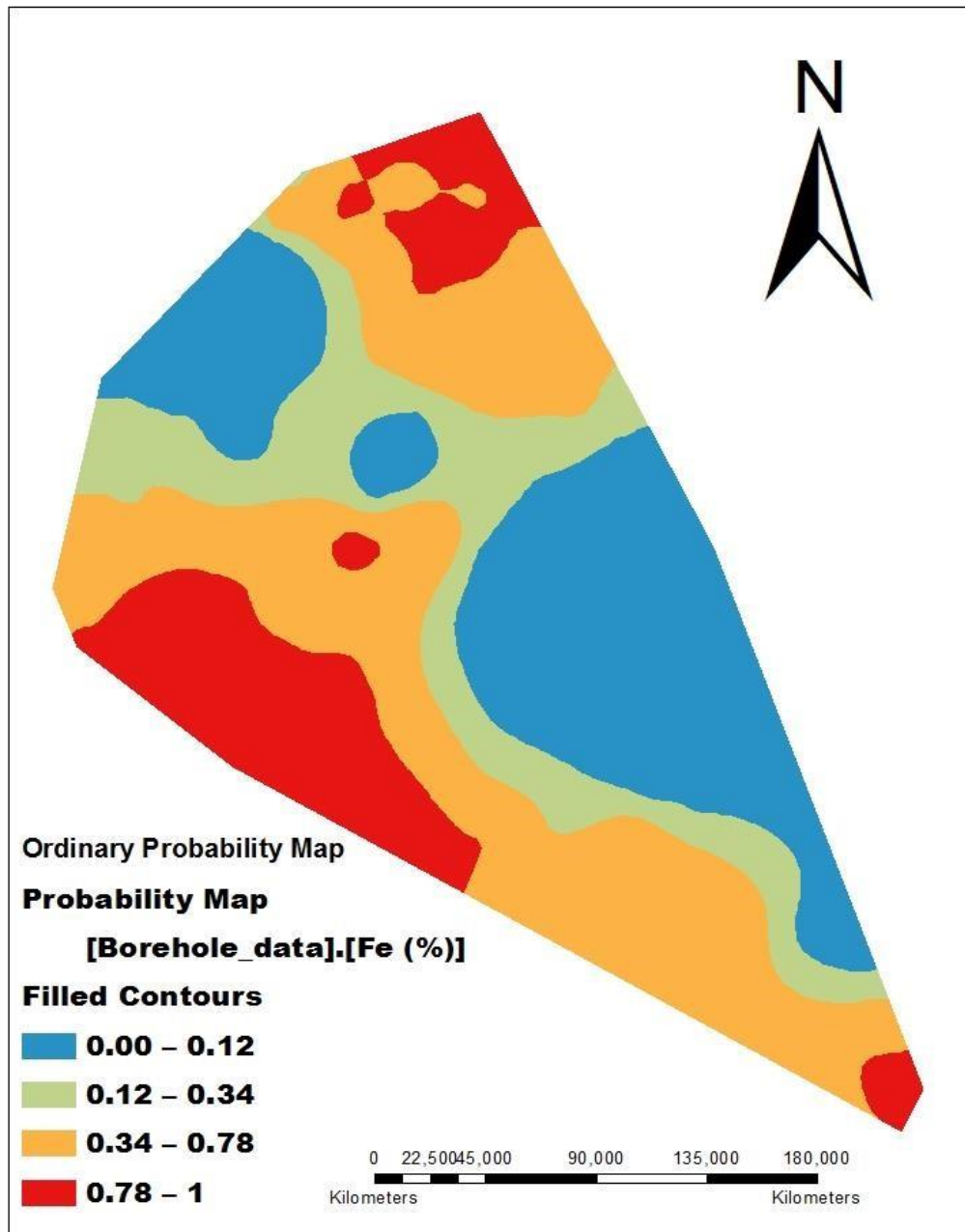


Figure 4.9: Ordinary Kriged Probability Map

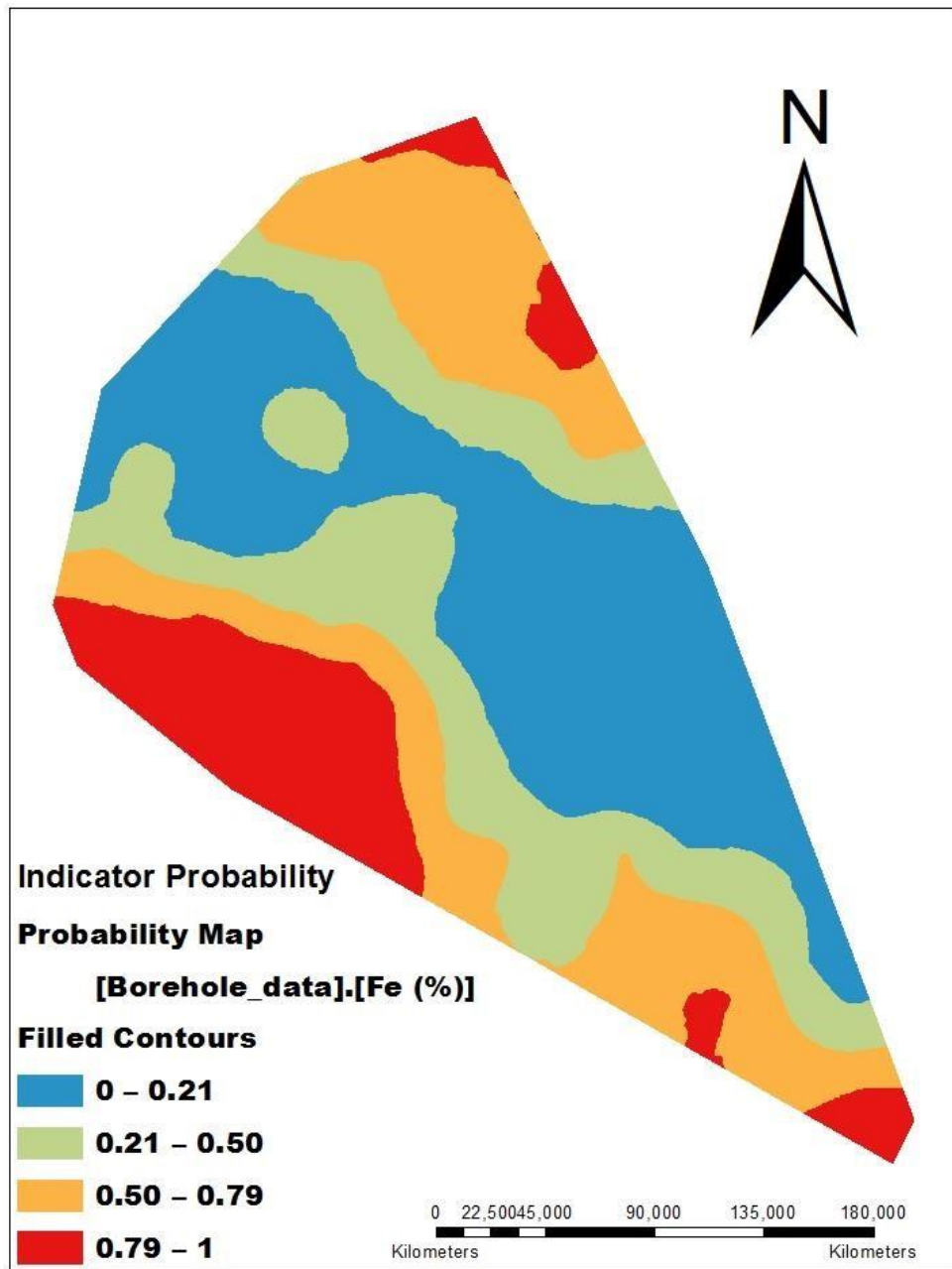


Figure 4.10: Indicator Kriged Probability Map

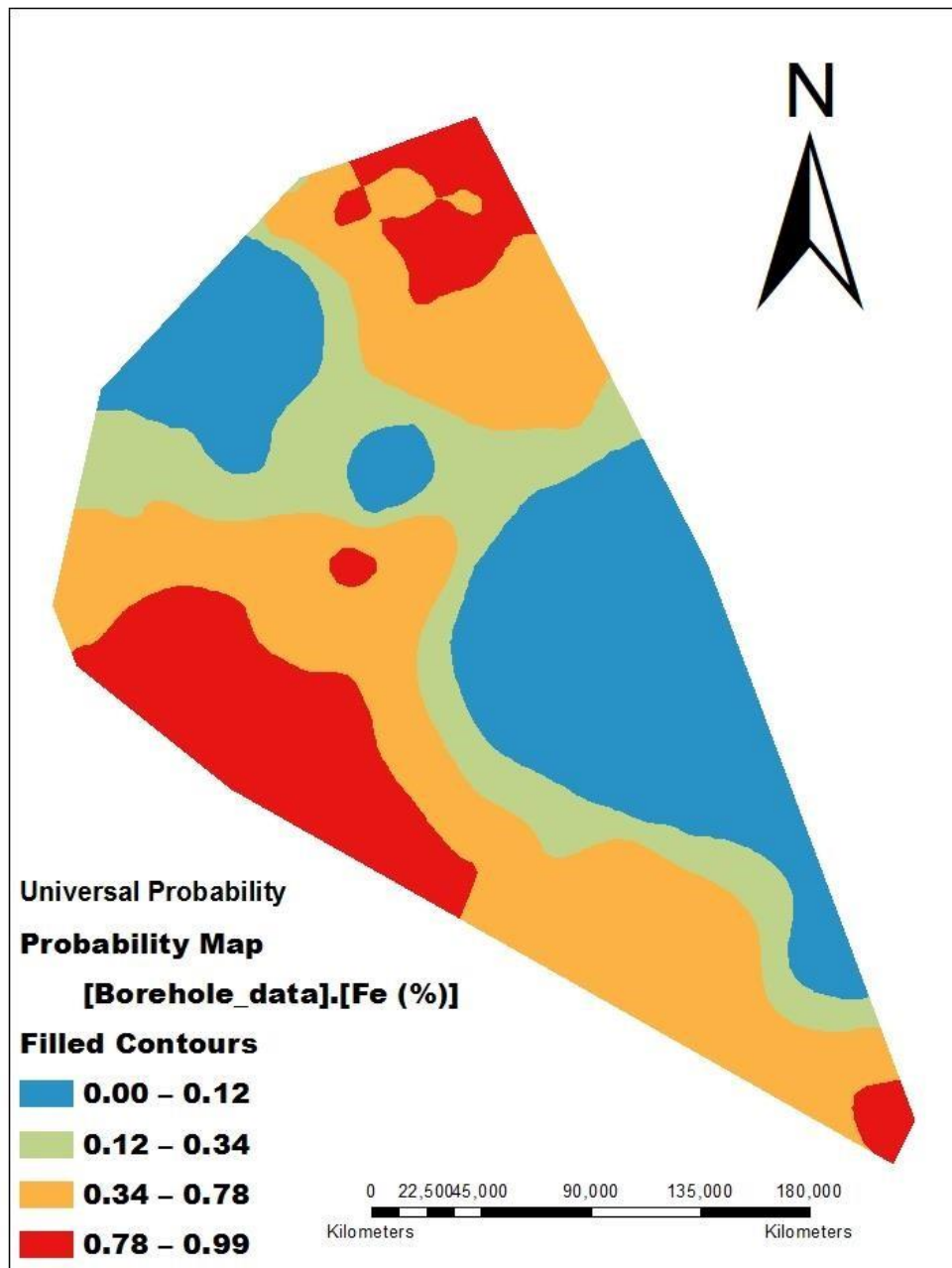


Figure 4.11: Universal Kriged Probability Map

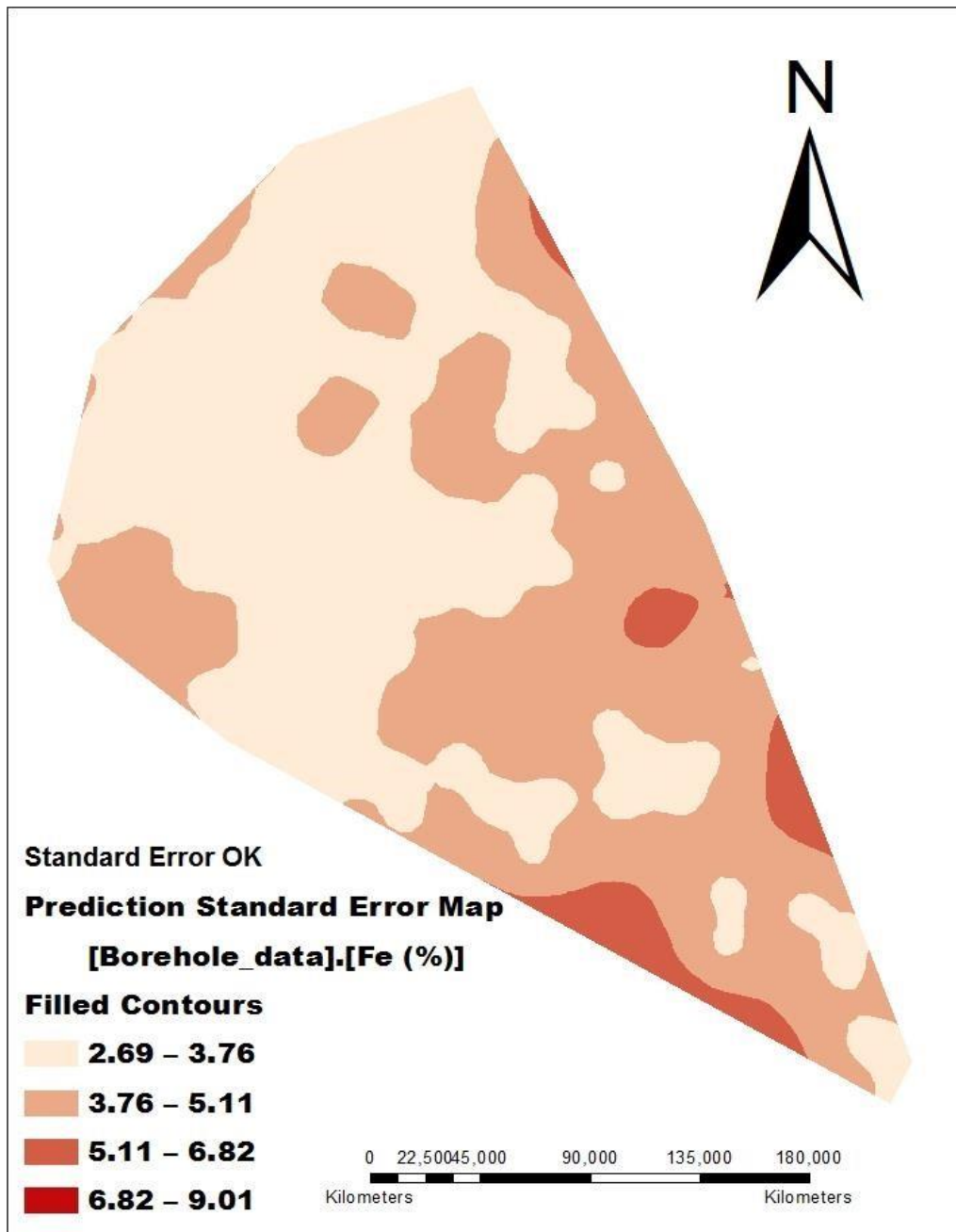


Figure 4.12: Ordinary Kriged Standard Error

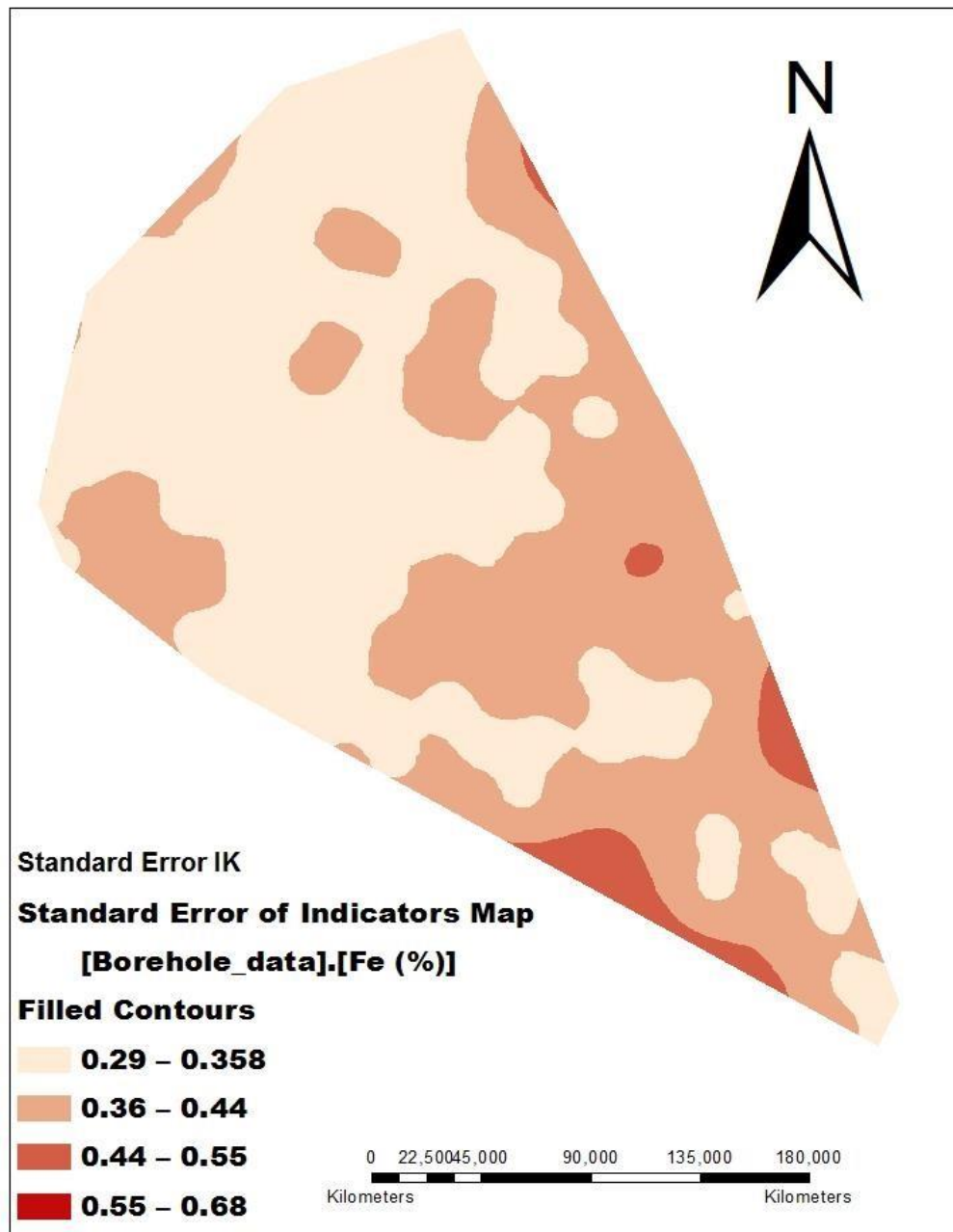


Figure 4.13: Indicator Kriged Standard Error

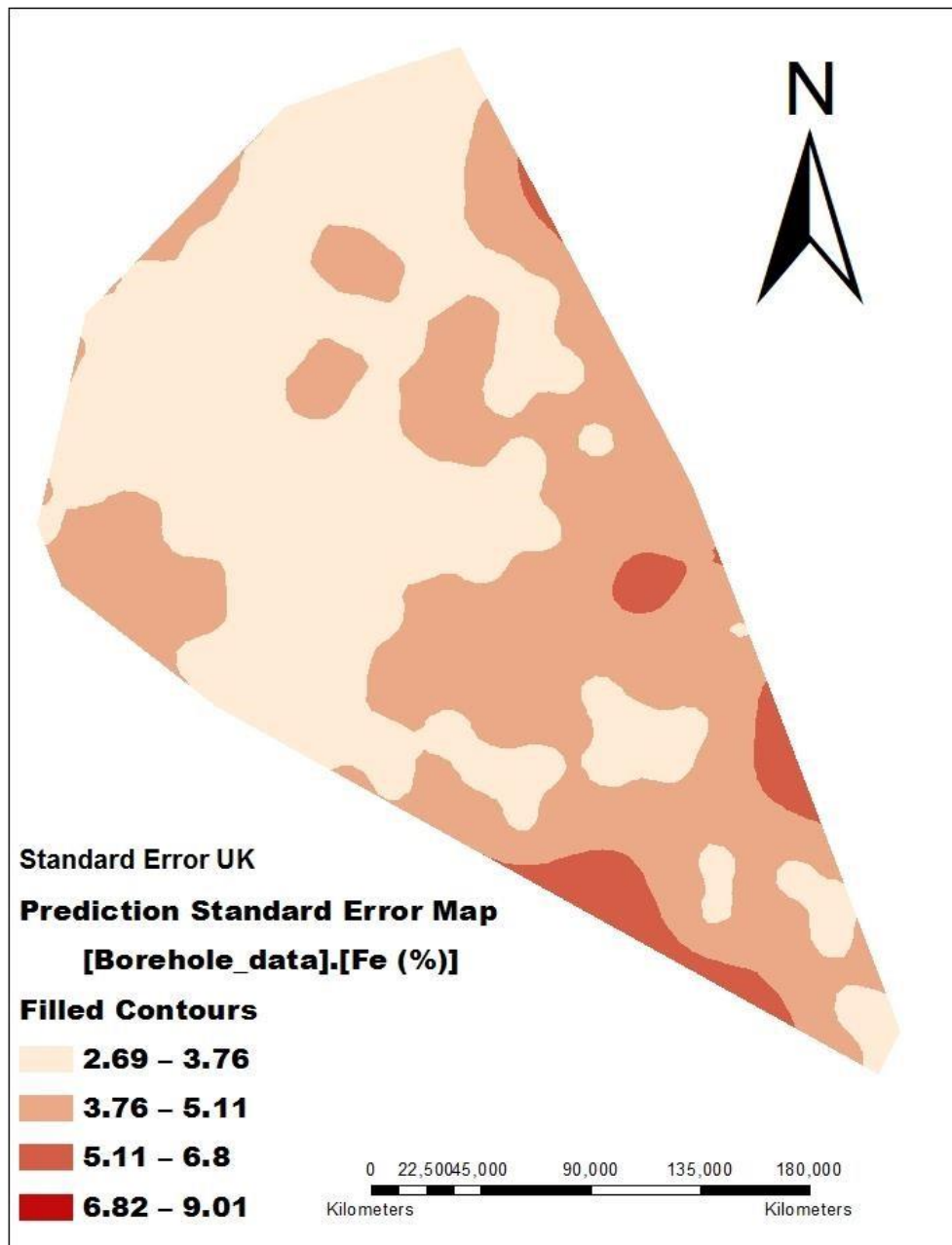
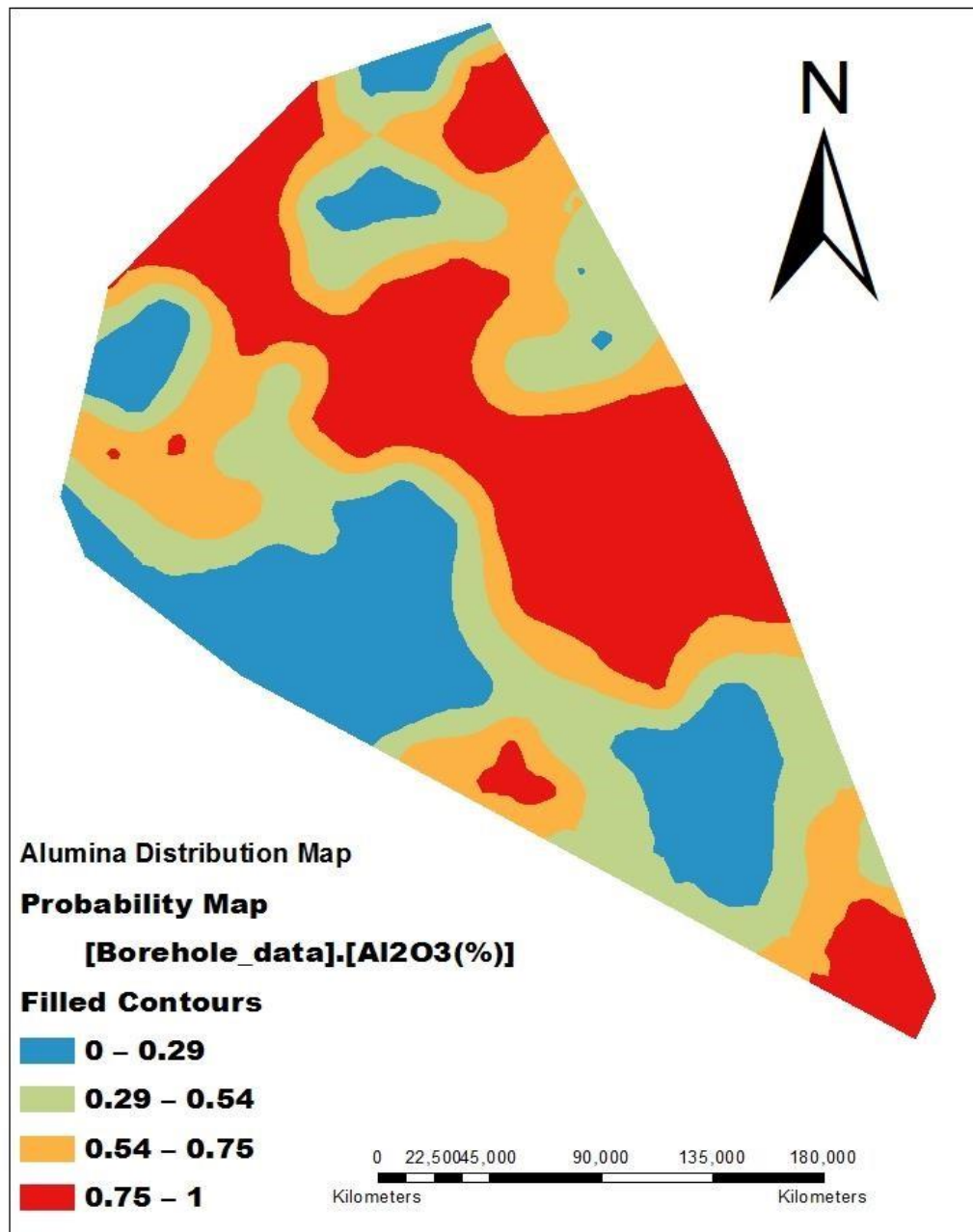


Figure 4.14: Universal Kriged Standard Error

Figure 4.15 and 4.16 show the Alumina and Silica distribution maps. From the color delineation, in which the red shows the alumina and silica concentrations in both maps.



Figures 4.15 Alumina distribution map

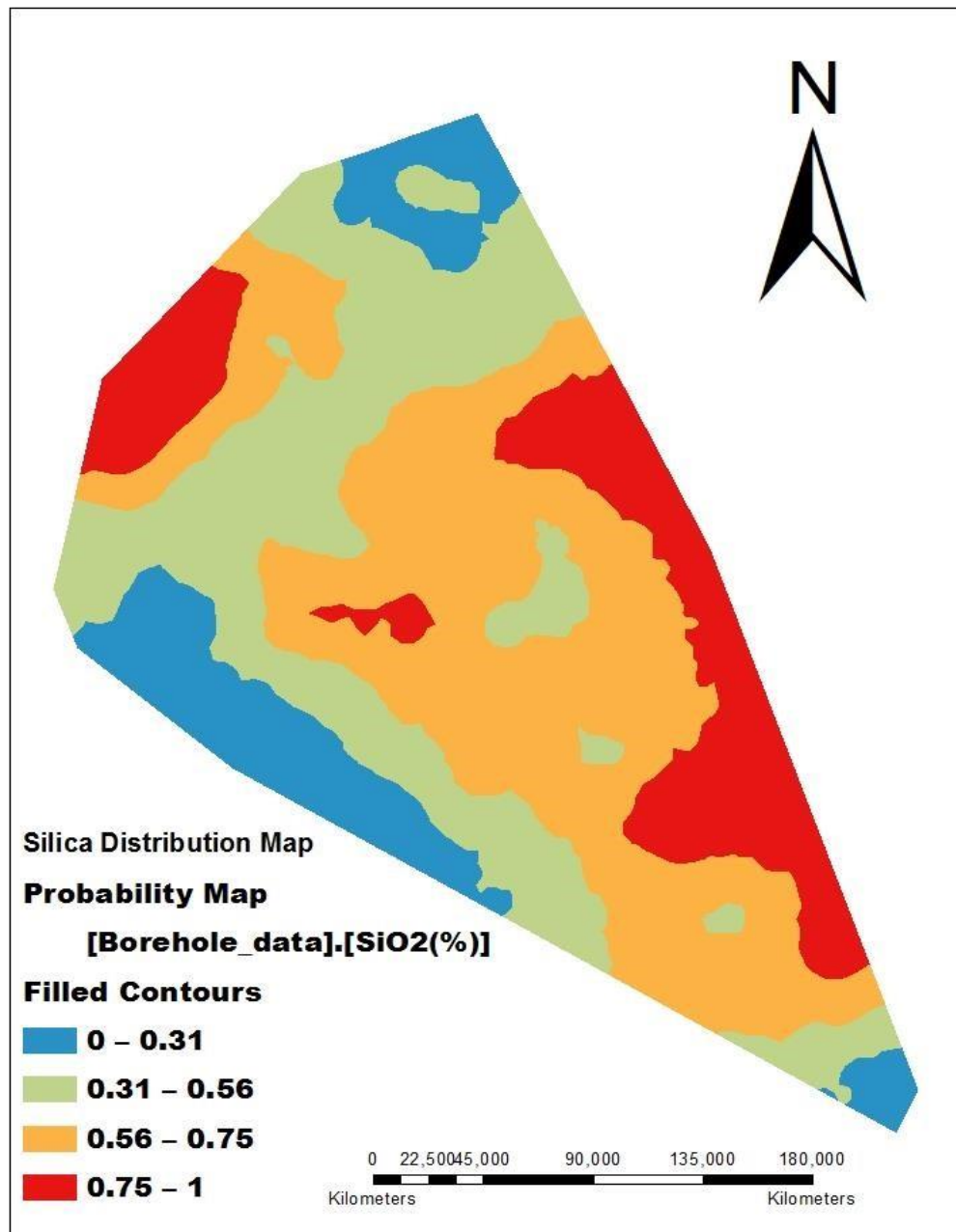


Figure 4.16: Silica Distribution Map

Figure 4.17 shows the 3D view of the bore holes and the linear distribution of the dataset generated from the Voxler software. These results when overlaid with the kriged maps validate the output surface maps generated from kriging interpolations.

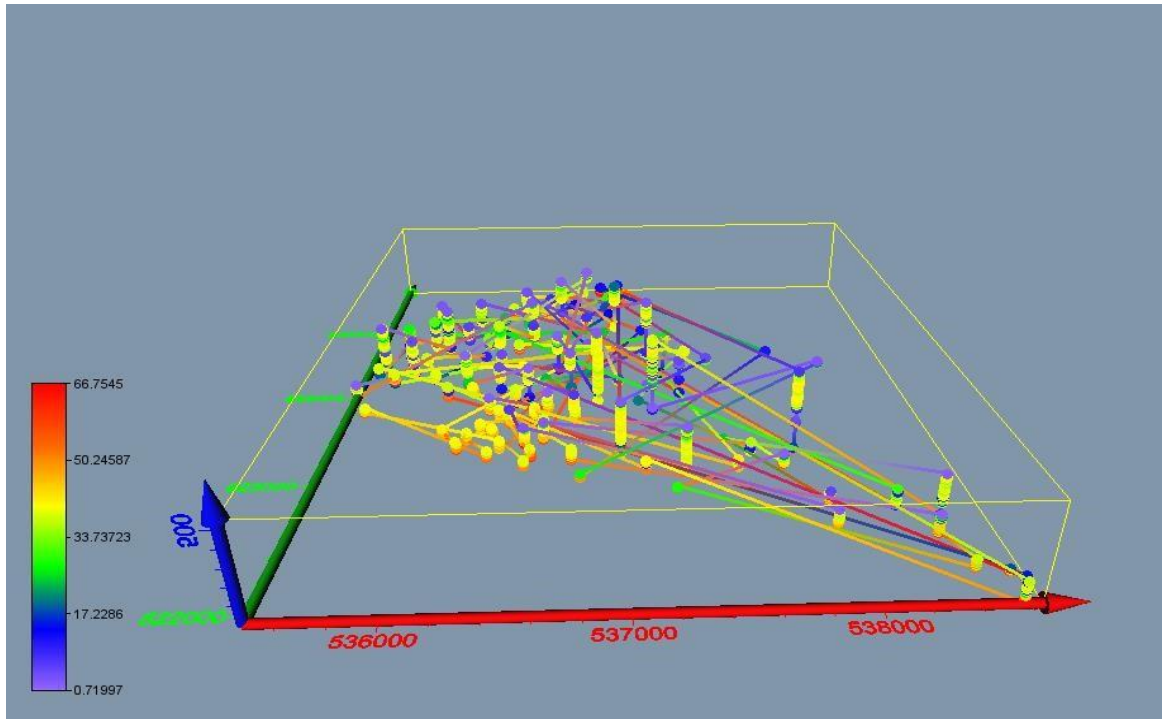


Figure 4.17: 3D view of the bore holes

CHAPTER 5

CONCLUSION AND RECOMMENDATION

5.1 Conclusion

Integrated method using Kriging in GIS is introduced and implemented in this work to establish the prospect of using this procedure in mapping the spatial distribution of iron, silica and aluminum content of iron ore at Mt. Tokadeh mining area. IK, OK, and UK were examined to select the most suitable technique for interpolating data obtained from the study site. Economical mining grades of iron ore were selected among poor areas. Application of GIS was used to support the visualization of the results and was also found to add more valuable information to the kriged result. Such integration enhances and reveals the mineral distribution and enables better mining decision, management and planning in the study area.

The following are the conclusion drawn from this work:

1. Geostatistical interpolation technique, mostly kriging is effective and efficient when integrated with GIS. After examining and validating the three interpolation techniques in kriging, IK was the best suited for the dataset and gives better prediction than OK and UK.
2. To better understand the magnitude of each mineral type, four classes of colors were used to delineate the mineral distributions, which show the iron, silica and alumina concentrations.
3. Indicator kriging was suitable in selecting mining site as High Grade or direct Shipping Ore (DSO). Setting the threshold at 25%, it shows that the northern and southern part of the study area were economically viable, while the center of the study area was concentrated with impurity as shown in Figure 4.7. However it also shows that some portion of the northern corner and south western corner of the study area were High Grade or Direct Shipping Ore at 40% threshold and if processed further its quality may increase to 65% iron.
4. The spatial distribution was generated in three output maps (Prediction map, Prediction Error map and Probability map)
5. Exponential semivariogram was proven to be the best suited. It removes the nugget effect making the prediction unbiased.

5.2 Recommendation

The followings are recommendation for future research:

1. Further research should focus on using this methodology to generate a database that can be updated and is capable of generating mineral distribution map.
2. The volume of minerals in selected mining site (High Grade or DSO) should also be calculated

3. This procedure should be examined on other ore reserves such as Bauxite, Gold and Manganese, etc.

KNUST

REFERENCES

- Amikiya, C.A., (2014). “Characterization of Iron Ore a Case Study of Mount Tokadeh, Western Nimba Area”, Liberia, published student thesis, Accessed January 15, 2016
- Bezzi, M. & Vitti, A., (2005) “A comparison of some kriging interpolation methods for the production of solar radiation maps”. *Geomatics Workbooks Vol. 5 - 6th Italian GRASS users meeting proceedings, Roma, 14-15 April, 2005*, pp.1–17.
- Bohling, G., (2005a) “Kriging”, pp.1–20, Accessed February 2, 2016.
- Bohling, G., (2005b), “Introduction to geostatistics and variogram analysis”, *Earth*, pp.1–20, Accessed March 12, 2015.
- Bonaventura, L. et al., (2005), “Random notes on kriging : an introduction to geostatistical interpolation for environmental applications”, pp.1-28, Accessed March 4, 2016.
- Boogaart, K.G. van den & Brenning, A., (2001), “Why Universal Kriging is better than IRFk-Kriging : Estimation of Variograms in the Presence of Trend” *Journal of Earth System Science*, pp.1–15.

- Brus, D.J. & Heuvelink, G.B.M., (2007), “Optimization of sample patterns for universal kriging of environmental variables”, *Geoderma*, 138(1-2), pp.86–95.
- Carlson, R.E. & Natarajan, B.K., (1994), “Sparse approximate multiquadric interpolation”, *Computers and Mathematics with Applications*, 27(6), pp.99–108.
- Carr, M.S. & Dutton, C.E., (1959), “Iron-Ore Resources of the United States Including Alaska and Puerto Rico”, *Geological Survey Bulletin 1082-C*, pp.6-78, Accessed March 4, 2015.
- Chadwick, J., (2011), “A fifth of Africa”, pp. 2-4, Accessed March 15, 2016.
- Chen, F.W. & Liu, C.W., (2012), “Estimation of the spatial rainfall distribution using inverse distance weighting (IDW) in the middle of Taiwan”, *Paddy and Water Environment*, 10(3), pp.209–222.
- Childs, C., (2004), “Interpolating Surfaces in ArcGIS Spatial Analyst”, *ArcUser*, Available at: www.esri.com, pp.1-4, Accessed on October 16, 2016.
- De Smith, M. J., Goodchild, M. F., Longley, P. A., (2005), “Geospatial Analysis”, *A comprehensive guide to principles, techniques and software tools, 5th Edition*, pp.1-144, Accessed on February 18, 2016.
- Dimitrakopoulos and Roussos (2012).” Ore Reserve Estimation and Strategic Mining Planning”, Available; <http://www.Springer.com>
- Drolq, G.E.D.Q.G. et al., (2015), “Study of Cu(II) Adsorption by Siderite and Kaolin”, *World Multidisciplinary Earth Sciences symposium, WMESS 2015.* , 15, pp.821–826.
- Dubrulle, O., (2003), “Geostatistics for Seismic Data Integration in Earth Models”, *Distinguished Instructor series, No.6*, pp.10-273, Accessed April 12, 2015.
- Environmental Protection Agency of Slovenia (2010), “Use of SAGA GIS for interpolation (Kriging)”, Prepared for 1st DMCSEE-TCP Training, Budapest,

2nd -5th February, pp.2–5, Accessed February 2, 2016

Everett, J.E., (2013), “Planning an Iron Ore Mine: From Exploration Data”, *Issues in Informing Science and Information Technology*, 10, pp.145–162.

Fu-cheng, L.I.U., Jun, P. & Cun-yong, Z., (2012), “A non-parametric indicator Kriging method for generating coastal sediment type map”, *Marine Science Bulletin*, 14(1).

Grant, M., (1990), “The Application of Kriging in the Statistical Analysis of Anthropometric Data”, *Air Force Institute of Technology, Air University, USA*, Published MSc. Thesis, Accessed April 12, 2015.

Hadden, B.R.L., (2006), “The Geology of Liberia : a Selected Bibliography of Liberian Geology”, *Geography and Earth Science*, (May), pp.5–6.

Hammah, R.E. & Curran, J.H., (2006), “Geostatistics in Geotechnical Engineering: Fad or Empowering?” *GeoCongress 2006*, pp.1–5.

Hardy, R.L., (1992), “A contribution of the multiquadric method: Interpolation of potential inside the earth $a(X,Y)$ ”, *Computers and Mathematics with Applications*, 24(12), pp.81–97.

Hengl, T., (2009), “A Practical guide to Geostatistical Mapping”, Available at: http://book.spatial-analyst.net/system/files/cover_geostat_2009.pdf, Accessed June 8, 2015.

Honerkamp, J., (2012), “Random Variables : Fundamentals”, Available at: https://www.google.com.gh/search?sclient=psyb&biw=1366&bih=623&q=Principle+of+Random+Variable+PDF&oq=Principle+of+Random+Variable+PF&gs_l. Accessed June 8, 2015.

Huang, C.L., Wang, H.W. & Hou, J.L., (2015), “Estimating spatial distribution of daily snow depth with kriging methods: combination of MODIS snow cover

area data and ground-based observations”, *The Cryosphere Discussions*, 9(5), pp.4997–5020.

Kambhammettu, B.V.N.P., Allena, P. & King, J.P., (2011), “Application and evaluation of universal kriging for optimal contouring of groundwater levels”, *Journal of Earth System Science*, 120(3), pp.413–422.

Kameshwara Rao, V. & Narayana, A.C., (2015), “Application of nonlinear geostatistical indicator kriging in lithological categorization of an iron ore deposit”, *Current Science*, 108(3), pp.413–421.

Kao, C.Y.S. & Hung, F.L.P., (2004), “Twelve Different Interpolation Methods : a Case Study”, *Proceedings of the XXth ISPRS Congress*, 35, pp.778–785.

Kastelec, D. & Košmelj, K., (2002), “Spatial Interpolation of Mean Yearly Precipitation using Universal Kriging”, *Metodološki zvezki*, (17), pp.149–162.

Kiptarus, J. J., Muumbo, A. M., Makokha, A. B., Kimutai, S. K., (2015), “Characterization of selected mineral ores in Eastern Zone of Kenya: Case study of Mwingi North Constituency in Kitui County”, *International Journal of Mining Engineering and Mineral Processing*, pp.8-17, Accessed October 16, 2016.

Krivoruchko, K., 2004. Introduction to Modeling Spatial Processes Using Geostatistical Analyst. Esri, pp.1–27. Available at: <http://www.esri.com/library/whitepapers/pdfs/intro-modeling.pdf>, Accessed on June 8, 2015.

Kumar, V., (2007), “Optimal contour mapping of groundwater levels using universal kriging—a case study”, *Hydrological Sciences Journal*, 52(February 2015), pp.1038–1050.

- Liberty, E.T., (2008), “Government of the Republic of Liberia 2008 national population and housing census : Preliminary result”, Available at:
[unstats.un.org/ unsd/ dnss/docViewer.aspx?docID=2075CachedSimilar](http://unstats.un.org/unsd/dnss/docViewer.aspx?docID=2075CachedSimilar).
- Lopez, C. & Samper, J., (2007), “Numerical Aspects of the Universal Kriging Method for Hydrological Applications” , (1984), pp.1–12. Available at:
<http://citeseerx.ist.psu.edu/viewdoc/download?doi=10.1.1.4.6646&rep=rep1&type=pdf>, Accessed on April 16, 2016.
- Ly, S., Charles, C. & Degré, A., (2011), “Geostatistical interpolation of daily rainfall at catchment scale: the use of several variogram models in the Ourthe and Ambleve catchments”, Belgium. *Hydrology and Earth System Sciences*, 15(7), pp.2259–2274.
- Lyon, S.W. et al., (2006), “Defining probability of saturation with indicator kriging on hard and soft data”, *Advances in Water Resources*, 29(2), pp.181–193.
- Matheron, G., (1971), “The Theory of Regionalized Variable and its Applications”, *Ecole Nationale Supérieure des Mines de Paris*, pp.8-218.
- Menafoglio, A., Grujic, O. & Caers, J., (2016), “Universal Kriging of functional data: Trace-variography vs cross-variography? Application to gas forecasting in unconventional shales”, *Spatial Statistics*. Pp. 2-22.
- MFA, (2003), “Environment Protection and Management Law of Liberia”, Available at:
www.unesco.org/culture/natlaws/media/pdf/liberia/liberia_act2002_engorof.pdf. Accessed on July 3, 2016.
- MLME, (2010). “Mineral Policy of Liberia, Monrovia”, Available at:
[www.eisourcebook.org/cms/June 2013/Liberia Mineral Policy.pdf](http://www.eisourcebook.org/cms/June_2013/Liberia_Mineral_Policy.pdf), Accessed on July 3, 2016.

- Poveromo, J.J. et al., (2000), "The making, Shaping and Treating of Steel", *11th Edition, Iron Making, Chapter 8*, pp.547–642.
- Rap, A., Ghosh, S. & Smith, M.H., (2009), "Shepard and Hardy Multiquadric Interpolation Methods for Multicomponent Aerosol–Cloud Parameterization", *Journal of the Atmospheric Sciences*, 66(1), pp.105–115.
- Ruiqing, D. & Jin, Y., (2012), "Application of Ordinary Kriging Method in Data Processing of Magnetic Survey", *Science & Education, (Iccse)*, pp.771–774.
- Saleem, H. A., (2007), "Integrated Methodology Using Geostatistics and GIS for Mining Evaluation: A case study of El Mahamid Area, Eyget", Published MSc. Thesis, Accessed on January 27, 2015.
- Srinivasan, B.V., Duraiswami, R. & Murtugudde, R., (2008), "Efficient kriging for real-time spatio-temporal interpolation Linear kriging", *20th Conference on Probability and Statistics in Atmospheric Sciences*, 17th-21st January 2010, Atlanta Georgia, USA, pp.228–235.
- Sterling, D.L., (2003), "A Comparison of Spatial Interpolation Techniques For Determining Shoaling Rates of The Atlantic Ocean Channel Approved : A Comparison of Spatial Interpolation Techniques For Determining Shoaling Rates of The Atlantic Ocean Channel", *Virginia Polytechnic Institute and State University, C*, pp.1–94.
- Tolosana-delgado, R. et al., (2015), "Improving processing by adaption to conditional geostatistical simulation of block compositions", *The Journal of The South African Institute of Mining and Metallurgy*, Vol.115, pp.13–26.
- Tolosana-Delgado, R., Pawlowsky-Glahn, V. & Egozcue, J., (2008), "Simplicial Indicator Kriging", *Journal of China University of Geosciences*, 19(1), pp.65–71.

U.S.A. Environmental Protection Agency, (1994), "Extraction and Beneficiation of Ores and Minerals", *Resource Document: Iron, Vol.3*, pp.1-23, Accessed March 27, 2015.

Valev, G. & Kastreva, P.,(2010), "Analysis of the Problems of Interpolation in Gis Medium", *3rd International Conference on Cartography and GIS*, 15th – 20 January 2010, Nessebar, Bulgaria, Accessed on February 23, 2016.

Yves Buro, E. et al, (2009), "Technical Assistance in Mining and Metallurgy In Liberia", WRAP-UP Report Volume I of III May 2009, Accessed on May 17, 2016.

